

## A 3D digital atlas of *C. elegans* and its application to single-cell analyses

Fuhui Long, Hanchuan Peng, Xiao Liu, Stuart K Kim & Eugene Myers

Supplementary figures and text:

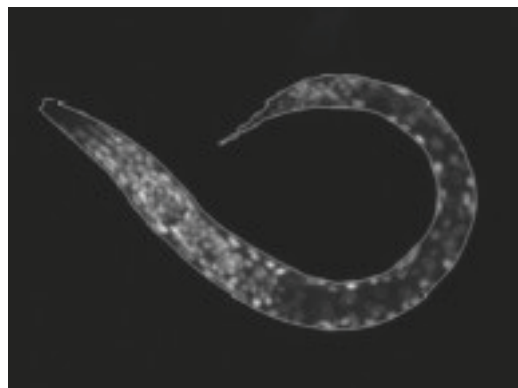
|                               |                                                                                                                                                  |
|-------------------------------|--------------------------------------------------------------------------------------------------------------------------------------------------|
| <b>Supplementary Figure 1</b> | Worm body straightening.                                                                                                                         |
| <b>Supplementary Figure 2</b> | Illustration of the automated 3D nuclei segmentation steps.                                                                                      |
| <b>Supplementary Figure 3</b> | A snapshot of the interface of the 3D nuclei annotation and visualization tool VANO and the spread-sheet generated by annotation.                |
| <b>Supplementary Figure 4</b> | Arrangement of pharyngeal nuclei in newly hatched L1.                                                                                            |
| <b>Supplementary Figure 5</b> | The mean and standard deviations of the nuclear locations of 357 cells along DV and LR axes computed from 15 images of L1 hermaphrodites larvae. |
| <b>Supplementary Figure 6</b> | AP graph of all the 357 nuclei included in the atlas.                                                                                            |
| <b>Supplementary Table 1</b>  | The mean and standard deviations of the 357 nuclei along AP, DV, and LR dimensions                                                               |
| <b>Supplementary Note</b>     | Additional details of methods                                                                                                                    |

*Note: Supplementary Videos 1–3 and Supplementary Data 1–2 are available on the Nature Methods website.*

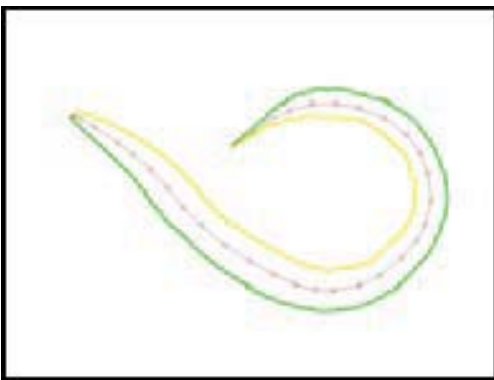
**Figure 1.** Worm body straightening. **(a)** A 3D image is projected to 2D by summing up all slices along Z. The detected boundary of the worm body is highlighted. **(b)** Estimated anterior-posterior (AP) axis (curve in red color) and dorsal/ventral sides (yellow and green curves). **(c)** Straightening the worm body in 3D by generating dense cutting planes orthogonal to the AP axis and then restacking the planes to make them parallel. **(d)** A single 2D slice of the 3D image after straightening.

# Supplementary Figure 1

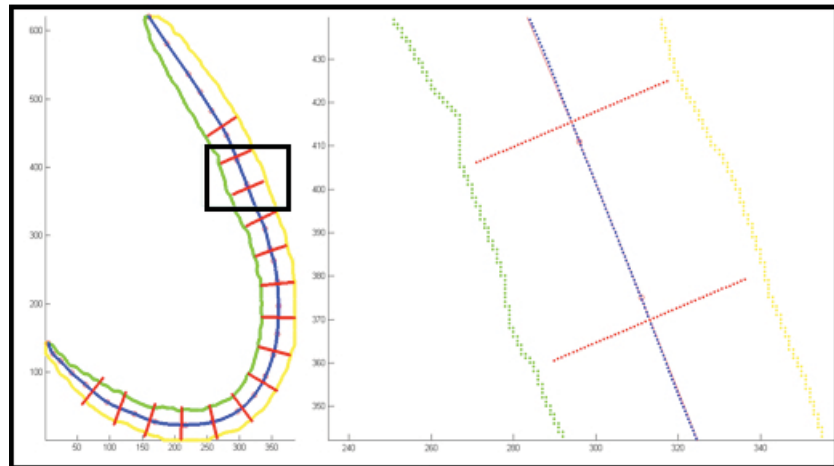
A



B



C



D

Nature Methods; doi: 10.1038/nmeth.1120

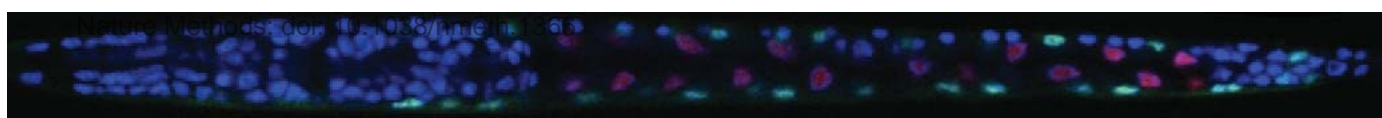
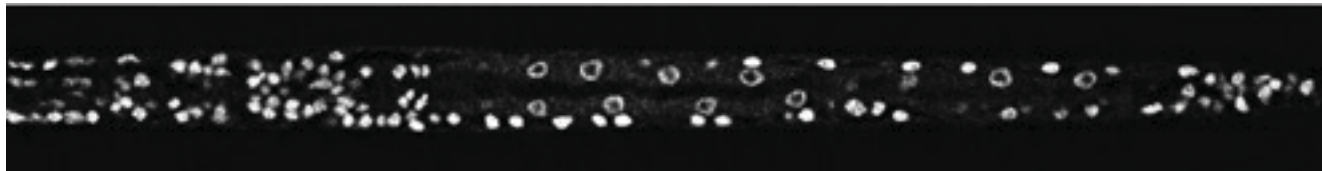


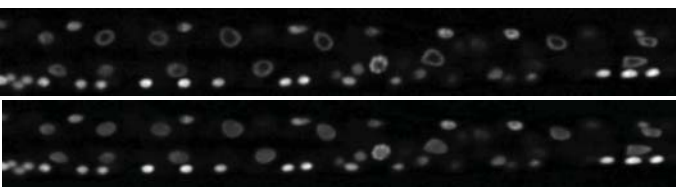
**Figure 2.** Illustration of the automated 3D nuclei segmentation steps. **(a)** A 2D slice of a 3D L1 worm image. **(b)** Before (upper panel) and after (lower panel) hole-filling. **(c)** The foreground mask (right) of a small portion of the head (left) obtained by adaptive thresholding. **(d)** An example of watershed segmentation (right). **(e)** Before (upper panel) and after (lower panel) merging over-segmented regions. **(f)** Before (upper panel) and after (lower panel) splitting under-segmented regions. **(g)** The contours of segmented nuclei overlaid on A.

## Supplementary Figure 2

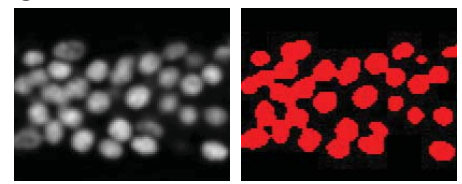
A



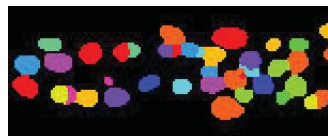
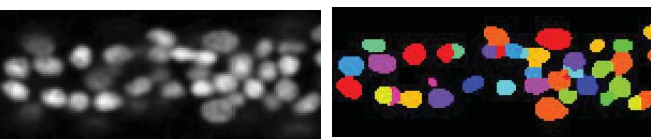
B



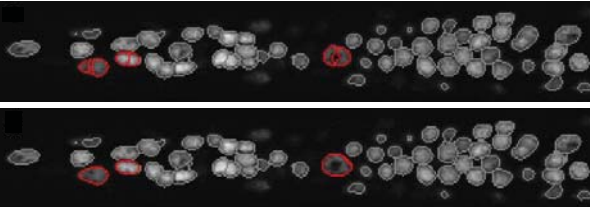
C



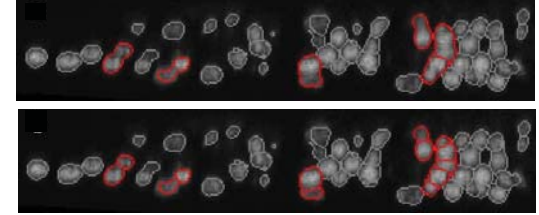
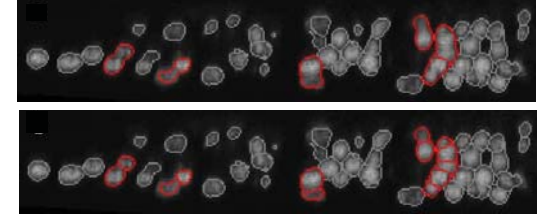
D



E



F



G

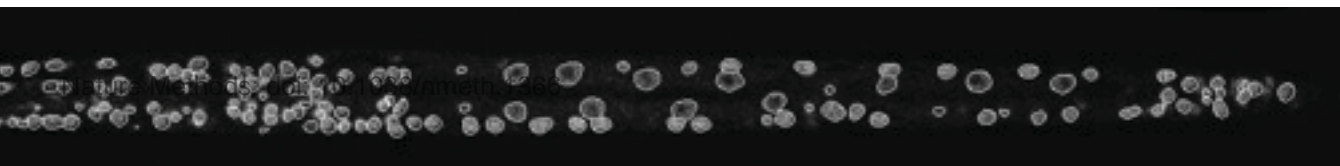
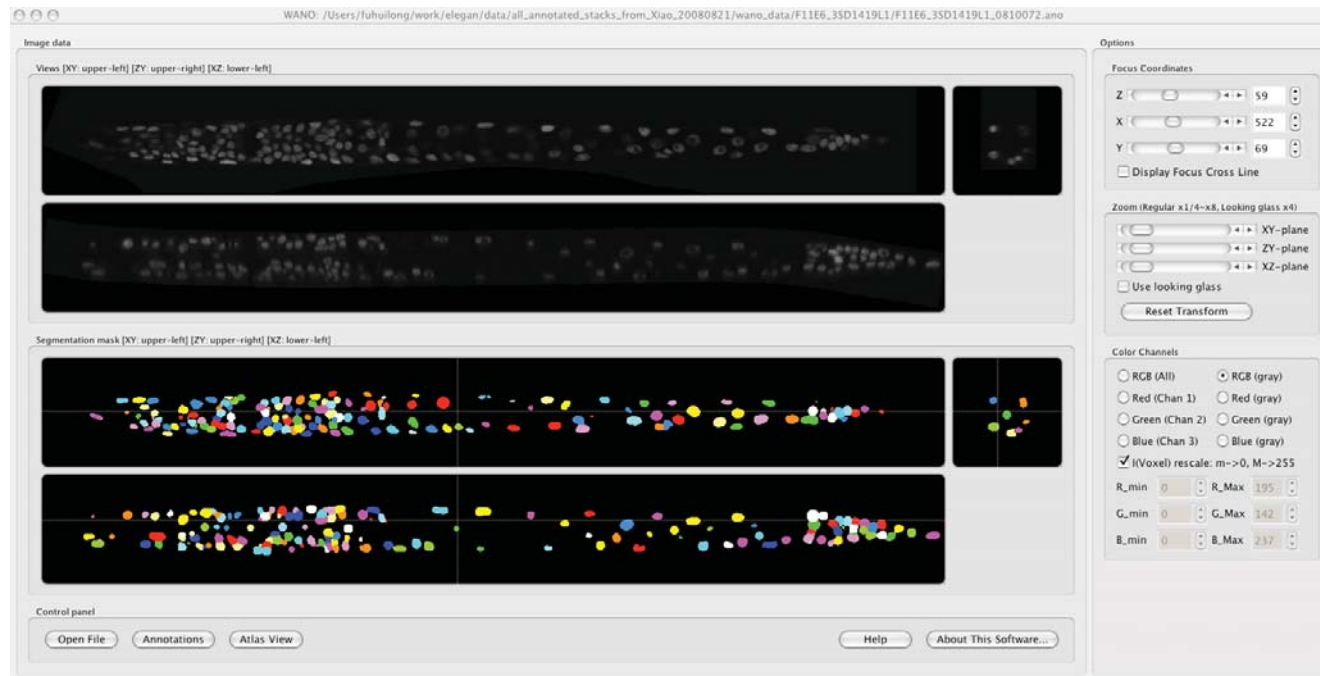


**Figure 3.** A snapshot of the interface of the 3D nuclei annotation and visualization tool VANO and the spread-sheet generated by annotation.

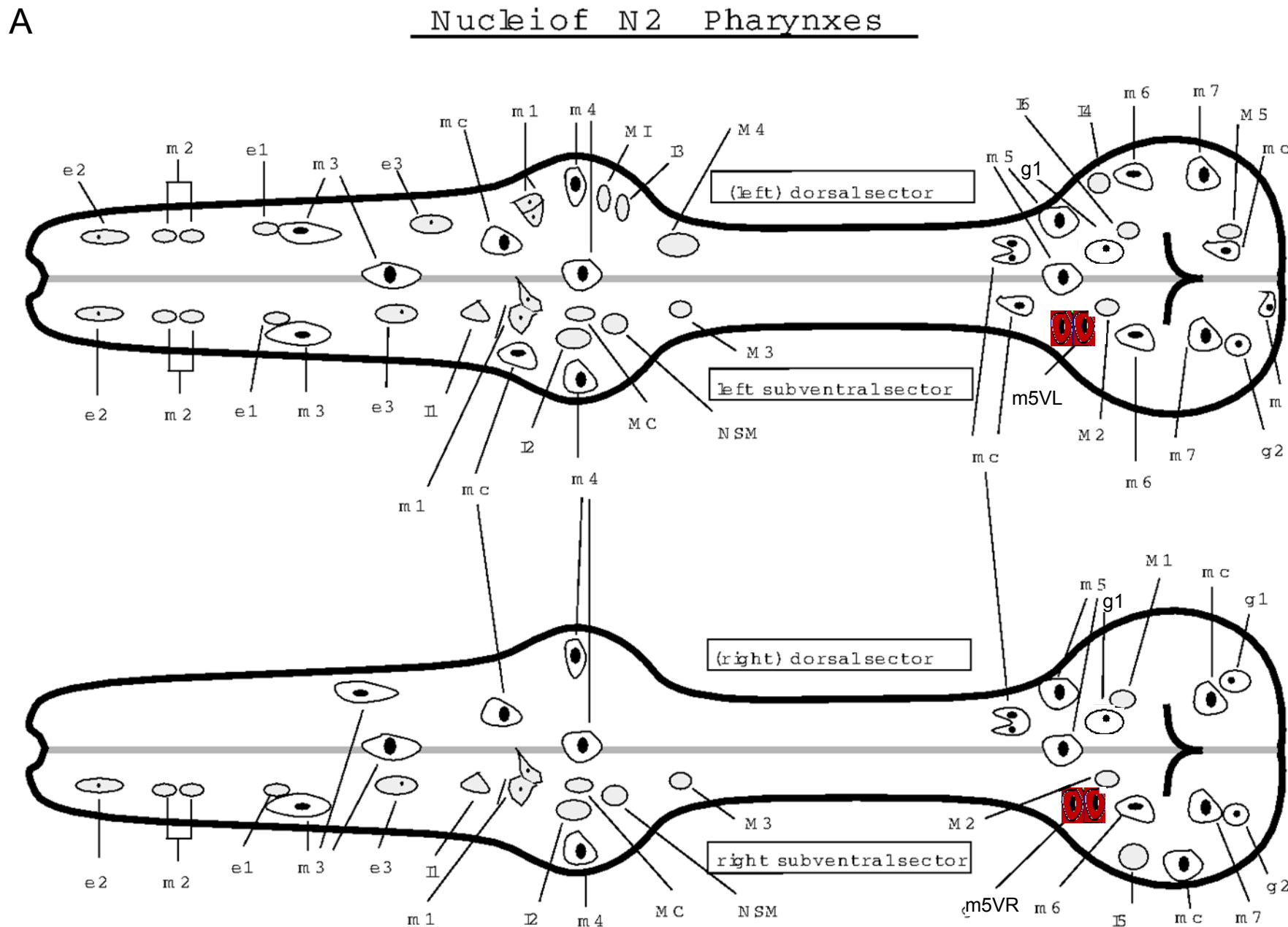
# Supplementary Figure 3

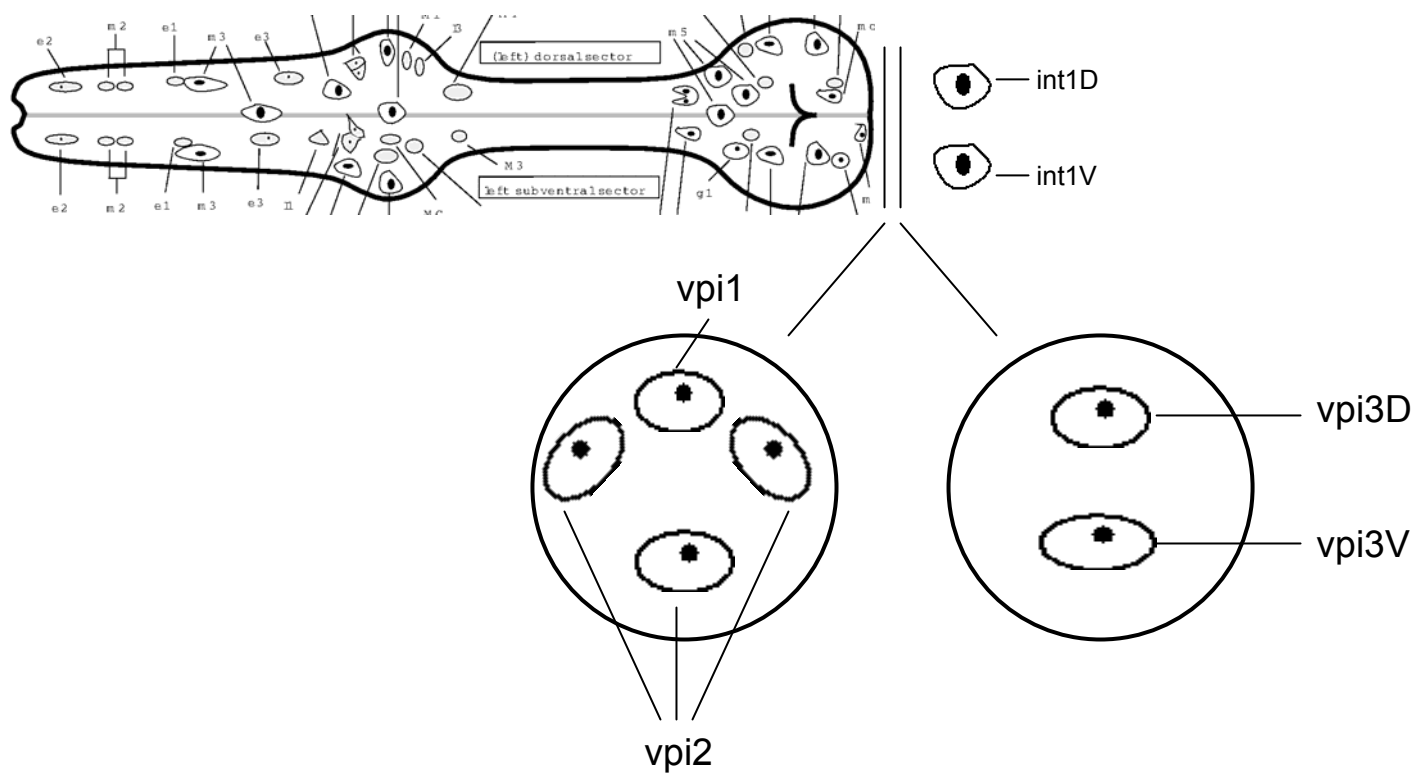


| Wano: Annotations in Tree |            |                |          |          |     |    |                |               |         |      |        |
|---------------------------|------------|----------------|----------|----------|-----|----|----------------|---------------|---------|------|--------|
| Order                     | Cell label | Name           | Comments | Z (page) | X   | Y  | Peak intensity | Ave Intensity | Std Dev | Size | Mass   |
| 85                        | 85         | MCR            |          | 65       | 184 | 76 | 189            | 88.18         | 37.81   | 1046 | 92241  |
| 86                        | 86         | hyp6 ABarpa... |          | 65       | 184 | 48 | 147            | 78.19         | 29.35   | 918  | 71777  |
| 87                        | 87         |                |          | 82       | 188 | 56 | 99             | 30.28         | 15.37   | 666  | 20166  |
| 88                        | 88         | bwmVR4         |          | 59       | 189 | 93 | 138            | 75.52         | 28.92   | 905  | 68348  |
| 89                        | 89         | pm4DL          |          | 68       | 189 | 58 | 171            | 95.01         | 28.48   | 1162 | 110396 |
| 90                        | 90         | I2R            |          | 59       | 189 | 82 | 194            | 124.53        | 29.98   | 530  | 66002  |
| 91                        | 91         | I2L            |          | 79       | 190 | 74 | 185            | 88.38         | 37.95   | 1780 | 157311 |
| 92                        | 92         | bwmVR          |          | 65       | 190 | 85 | 152            | 81.97         | 27.58   | 1067 | 87462  |
| 93                        | 93         | pm4IR          |          | 50       | 191 | 74 | 213            | 90.54         | 40.28   | 1027 | 92987  |
| 94                        | 94         |                |          | 53       | 191 | 86 | 216            | 100.55        | 53.06   | 746  | 75007  |
| 95                        | 95         | pm4L           |          | 81       | 192 | 65 | 150            | 70.34         | 25.36   | 1043 | 73366  |
| 96                        | 96         | bwmDR4         |          | 48       | 193 | 64 | 137            | 76.12         | 22.93   | 1059 | 80607  |

Nature Methods: doi:10.1038/nmeth.1366

**Figure 4.** Arrangement of pharyngeal nuclei in newly hatched L1. **(a)** Pairs of pharyngeal m2 nuclei have ambiguous cell lineage identities. For convenience, the anterior nucleus is denoted (l) and the posterior one is denoted (r). This figure is modified from [http://elegans.swmed.edu/Worm\\_labs/Avery/Pictures/RE\\_pharynx.gif](http://elegans.swmed.edu/Worm_labs/Avery/Pictures/RE_pharynx.gif). **(b)** Pharyngeal-intestinal valve cells, extrapolated from AlimFig1, <http://www.wormatlas.org/handbook/alimentary/alimentary2.htm>.

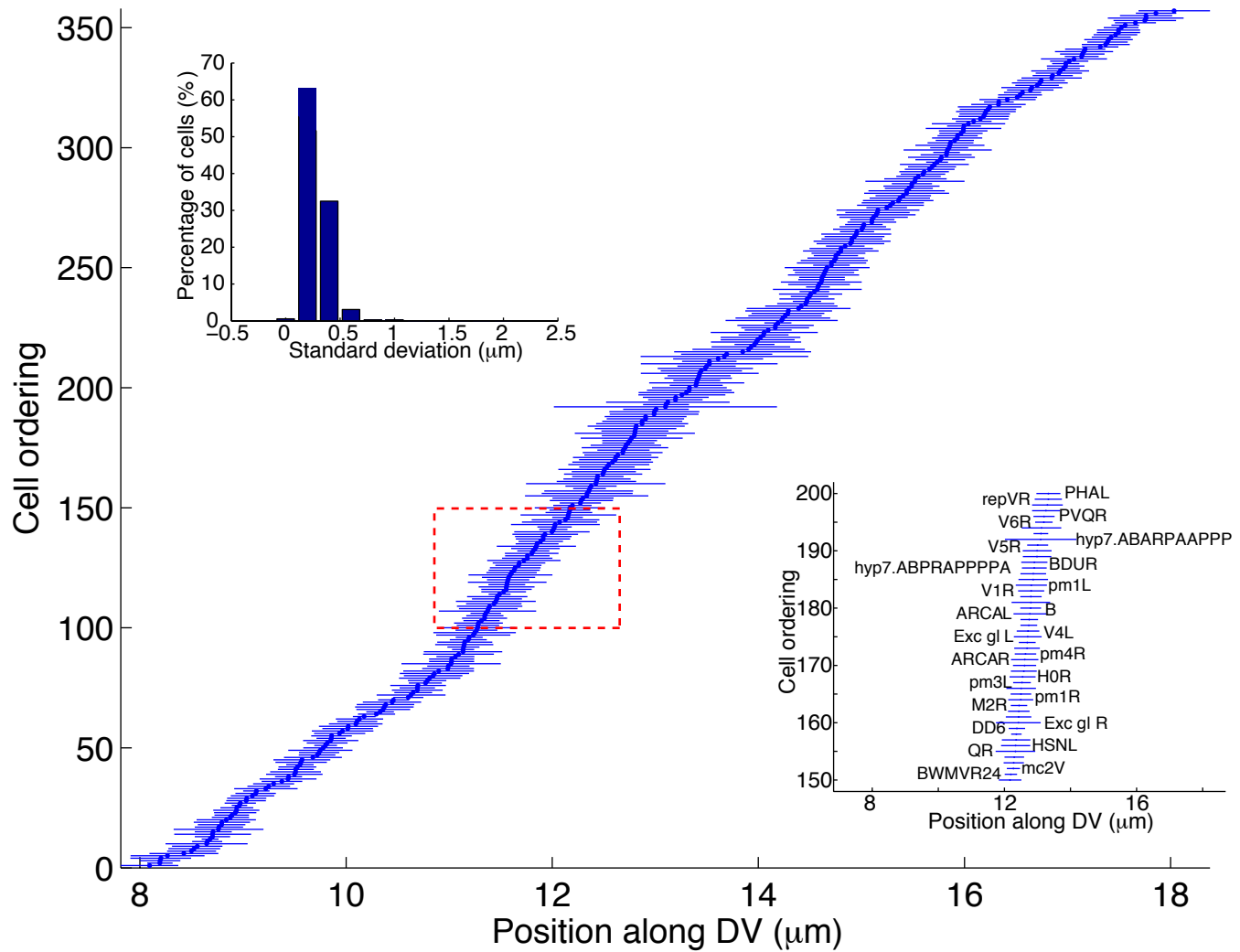


**B**

**Figure 5.** The mean and standard deviations of the nuclear locations of 357 cells along DV (**a**) and LR (**b**) axes computed from 15 images of L1 hermaphrodites larvae. The horizontal axis is the position of nuclei along DV (**a**) or LR (**b**) axes (in  $\mu\text{m}$ ), the dorsal side and right side being positive respectively. The vertical axis is the ordering of the nuclei sorted according to their mean locations along DV (**a**) or LR (**b**). The dots are the mean locations of the corresponding nuclei and the lines are their standard deviations. The bottom-right insets show the names of a subset of nuclei. The up-left insets show the distribution of the standard deviation of nuclei.

Supplementary Figure 5

A



Supplementary Figure 5

B

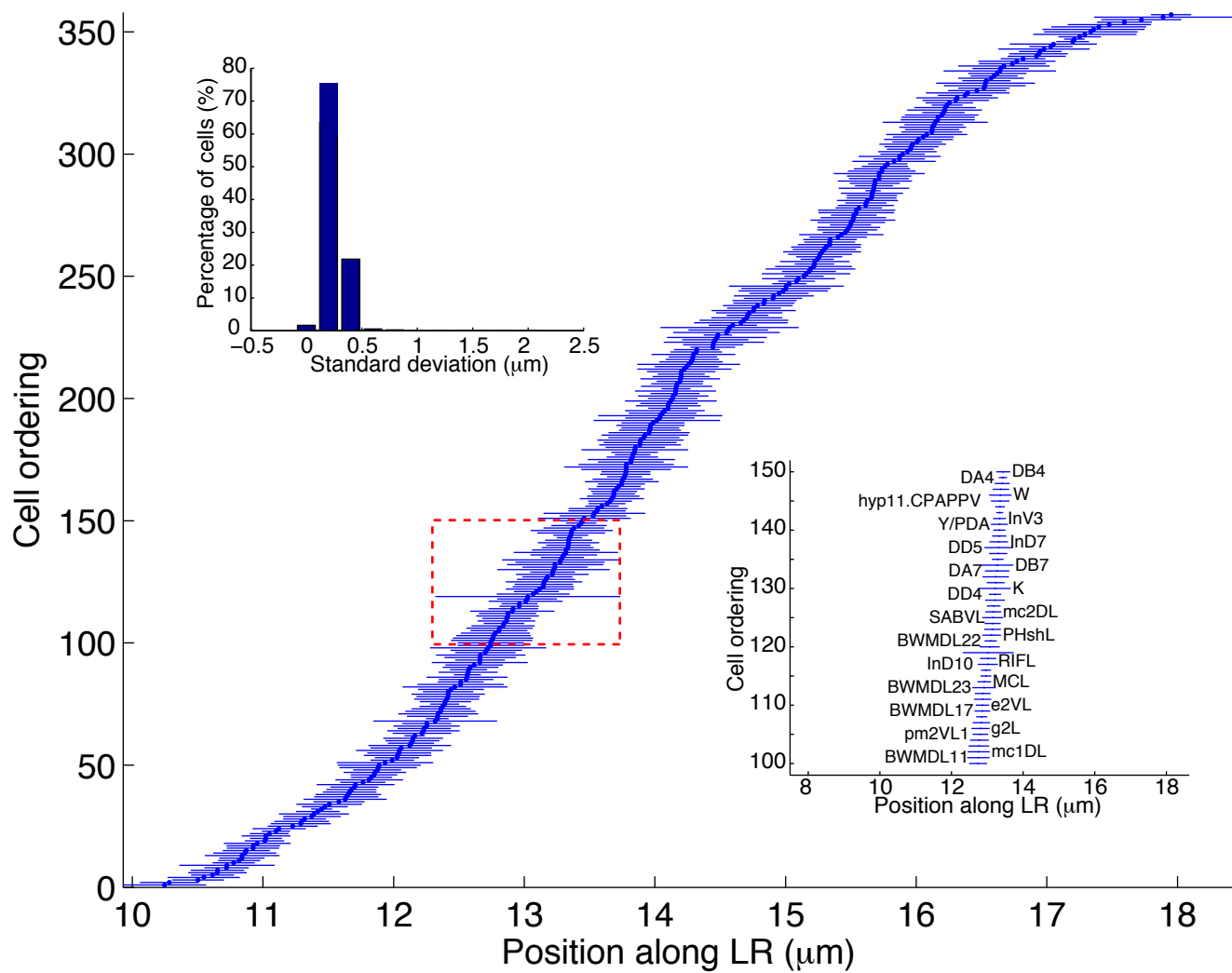


**Figure 6.** AP graph of all the 357 nuclei included in the atlas. The graph is displayed after transitive reduction. Thus if there is a directed path from node  $a$  to node  $b$ , and from node  $b$  to node  $c$ , then the transitively inferable edge from  $a$  to  $c$  is removed.



## **Supplementary Table 1**

The mean (columns 2 to 4) and standard deviations (columns 5 to 7) of the 357 nuclei along AP, DV, and LR dimensions. The unit is  $\mu\text{m}$ . A nuclei name converting table for these 357 nuclei is also attached at the end.

| Cell Name | mean of AP | mean of DV | mean of LR | std of AP | std of DV | std of LR |
|-----------|------------|------------|------------|-----------|-----------|-----------|
| AMshL     | 79.2892    | 15.3979    | 11.0345    | 4.5699    | 0.4924    | 0.4919    |
| AMshR     | 78.5207    | 15.4032    | 17.3936    | 4.5988    | 0.4376    | 0.3595    |
| Exc gl L  | 84.3402    | 12.8521    | 11.1337    | 2.7562    | 0.9934    | 0.321     |
| Exc gl R  | 85.0748    | 13.1296    | 16.9897    | 2.6249    | 1.2512    | 0.4254    |
| H0L       | 38.503     | 12.7032    | 10.8278    | 1.0009    | 0.5479    | 0.24      |
| H0R       | 38.4407    | 12.8258    | 17.6701    | 1.3584    | 0.6016    | 0.2842    |
| H1L       | 54.0933    | 12.6733    | 10.5231    | 1.7838    | 0.4837    | 0.2986    |
| H1R       | 54.5823    | 12.4906    | 17.6524    | 1.6542    | 0.6546    | 0.4452    |
| H2L       | 80.8515    | 13.3419    | 10.4817    | 2.768     | 0.6197    | 0.3405    |
| H2R       | 80.2052    | 13.1405    | 17.7454    | 2.8752    | 0.6624    | 0.4676    |
| P1/2L     | 105.1235   | 11.3266    | 10.8347    | 1.2636    | 0.4769    | 0.2223    |
| P1/2R     | 105.9381   | 11.0676    | 16.9702    | 1.2944    | 0.3564    | 0.2299    |
| P11/12L   | 187.4195   | 13.068     | 11.4788    | 2.384     | 0.5553    | 0.3852    |
| P11/12R   | 188.4221   | 12.4778    | 15.9975    | 1.4348    | 0.5406    | 0.309     |
| P3/4L     | 119.023    | 11.6927    | 10.9839    | 1.3515    | 0.3705    | 0.2531    |
| P3/4R     | 119.5913   | 11.2571    | 16.9111    | 1.1821    | 0.419     | 0.2292    |
| P5/6L     | 136.2896   | 11.9026    | 10.7792    | 1.6648    | 0.3933    | 0.2161    |
| P5/6R     | 134.0358   | 11.4247    | 16.6373    | 1.6819    | 0.4719    | 0.2968    |
| P7/8L     | 155.0697   | 11.9358    | 11.1463    | 1.1387    | 0.6276    | 0.2401    |
| P7/8R     | 153.0243   | 11.3378    | 16.0986    | 1.6993    | 0.5759    | 0.3131    |
| P9/10L    | 172.016    | 12.3132    | 11.5174    | 1.1476    | 0.4041    | 0.3005    |
| P9/10R    | 169.8823   | 11.6418    | 15.9816    | 2.1884    | 0.5219    | 0.3008    |
| QL        | 161.8539   | 13.375     | 11.4226    | 1.8664    | 0.684     | 0.2455    |
| QR        | 157.9274   | 12.4792    | 16.2754    | 2.3854    | 0.7056    | 0.2731    |
| V1L       | 98.5819    | 13.3298    | 10.8481    | 1.8035    | 0.5004    | 0.2601    |
| V1R       | 100.0654   | 12.7913    | 17.1507    | 1.4883    | 0.3633    | 0.3766    |
| V2L       | 111.7817   | 12.2995    | 10.8884    | 1.3043    | 0.3965    | 0.2234    |
| V2R       | 112.6251   | 11.8823    | 17.0743    | 1.0753    | 0.404     | 0.1833    |
| V3L       | 127.6555   | 12.5236    | 10.9628    | 1.2264    | 0.4539    | 0.2289    |
| V3R       | 127.7134   | 12.0482    | 16.775     | 1.1097    | 0.457     | 0.274     |
| V4L       | 147.9913   | 12.7666    | 11.0291    | 1.0667    | 0.5388    | 0.1987    |
| V4R       | 147.1731   | 12.3309    | 16.4861    | 1.4461    | 0.5905    | 0.3541    |
| V5L       | 168.2358   | 13.273     | 11.598     | 1.3457    | 0.5871    | 0.263     |
| V5R       | 166.5293   | 12.7655    | 16.2107    | 1.0258    | 0.4394    | 0.2152    |

|        |          |         |         |        |        |        |
|--------|----------|---------|---------|--------|--------|--------|
| V6L    | 178.5514 | 13.6903 | 11.5485 | 1.2667 | 0.6265 | 0.1774 |
| V6R    | 177.9455 | 13.1112 | 16.165  | 1.2452 | 0.4445 | 0.2293 |
| BWMVR1 | 30.2051  | 10.8939 | 16.6259 | 1.4332 | 0.5577 | 0.3125 |
| BWMDL1 | 30.2364  | 14.6142 | 11.9492 | 1.7692 | 0.4957 | 0.2741 |
| BWMDR1 | 30.3896  | 14.7454 | 16.5772 | 1.5345 | 0.4561 | 0.2205 |
| BWMVL1 | 30.2349  | 10.8502 | 11.7122 | 1.5538 | 0.5364 | 0.3421 |
| BWMVL2 | 34.2202  | 9.8617  | 11.9672 | 1.7403 | 0.3739 | 0.3601 |
| BWMDR2 | 34.5752  | 15.5788 | 16.2755 | 1.2125 | 0.4531 | 0.2063 |
| BWMDL2 | 34.5038  | 15.5386 | 12.3158 | 1.5035 | 0.4025 | 0.3021 |
| BWMVR2 | 34.1051  | 9.9245  | 16.1293 | 1.324  | 0.4166 | 0.3794 |
| BWMDR3 | 39.8387  | 16.2179 | 16.1831 | 1.9161 | 0.4153 | 0.3762 |
| BWMDL3 | 39.9062  | 16.1639 | 12.4308 | 1.6493 | 0.316  | 0.4419 |
| BWMVL3 | 39.5495  | 9.3094  | 12.1898 | 1.9406 | 0.2824 | 0.3044 |
| BWMVR3 | 39.3914  | 9.3069  | 15.8536 | 1.5065 | 0.3208 | 0.3639 |
| BWMVR4 | 46.1034  | 9.763   | 16.3916 | 1.5658 | 0.3383 | 0.3738 |
| BWMDL4 | 46.0471  | 15.8677 | 11.7771 | 1.566  | 0.3214 | 0.4454 |
| BWMVL4 | 46.6074  | 9.901   | 11.4416 | 1.4292 | 0.366  | 0.2426 |
| BWMDR4 | 46.281   | 15.8622 | 16.7947 | 2.0142 | 0.3707 | 0.2203 |
| BWMDR5 | 52.7785  | 16.8701 | 16.0776 | 1.5574 | 0.3772 | 0.3017 |
| BWMVL5 | 54.0738  | 9.2148  | 12.1031 | 1.4628 | 0.5038 | 0.2755 |
| BWMDL5 | 53.7371  | 16.9053 | 12.4625 | 1.8395 | 0.3466 | 0.4845 |
| BWMVR5 | 53.423   | 9.0914  | 15.6014 | 1.1897 | 0.3365 | 0.4105 |
| BWMVR6 | 56.865   | 9.7931  | 16.4565 | 1.375  | 0.368  | 0.4171 |
| BWMDL6 | 57.1763  | 16.4106 | 12.0041 | 2.2646 | 0.5035 | 0.4427 |
| BWMDR6 | 56.1835  | 16.4501 | 16.5026 | 2.1117 | 0.4073 | 0.4556 |
| BWMVL6 | 58.8442  | 9.9501  | 11.3909 | 2.1109 | 0.4212 | 0.3114 |
| BWMVR7 | 68.9902  | 8.9239  | 15.6659 | 1.4377 | 0.3705 | 0.3367 |
| BWMDR7 | 70.2763  | 17.6773 | 15.7149 | 1.6073 | 0.368  | 0.4327 |
| BWMDL7 | 73.2761  | 17.6802 | 12.811  | 2.8369 | 0.428  | 0.5874 |
| BWMVL7 | 71.9593  | 8.9924  | 12.145  | 3.1203 | 0.4174 | 0.2436 |
| BWMVR8 | 79.4071  | 9.4042  | 16.0092 | 2.8789 | 0.3104 | 0.2849 |
| BWMVL8 | 80.3263  | 9.6401  | 11.8696 | 2.6859 | 0.3434 | 0.2669 |
| BWMDL8 | 80.2072  | 17.4042 | 12.282  | 2.8889 | 0.3713 | 0.4585 |
| BWMDR8 | 77.0335  | 17.4676 | 16.4091 | 2.9269 | 0.2998 | 0.4452 |
| BWMVR9 | 84.1651  | 9.3094  | 15.5545 | 1.6727 | 0.3667 | 0.2532 |
| BWMVL9 | 85.6463  | 9.2735  | 12.3986 | 2.1612 | 0.4413 | 0.2563 |

|         |          |         |         |        |        |        |
|---------|----------|---------|---------|--------|--------|--------|
| BWMDL9  | 84.927   | 17.5751 | 12.9203 | 1.976  | 0.2811 | 0.4465 |
| BWMDR9  | 82.666   | 17.8261 | 15.8058 | 2.4419 | 0.2915 | 0.3942 |
| BWMDR10 | 87.1728  | 17.0045 | 16.4689 | 2.8788 | 0.2735 | 0.2926 |
| BWMVL10 | 91.9713  | 9.7545  | 11.7855 | 3.2538 | 0.2845 | 0.3809 |
| BWMDL10 | 91.5246  | 17.2283 | 12.3698 | 3.0518 | 0.3099 | 0.4865 |
| BWMVR10 | 90.3134  | 9.4419  | 15.7929 | 2.0458 | 0.2374 | 0.2497 |
| BWMDL11 | 100.91   | 17.5189 | 12.8379 | 1.7242 | 0.2157 | 0.4205 |
| BWMVR11 | 97.509   | 9.4935  | 15.3974 | 1.7206 | 0.2584 | 0.241  |
| BWMVL11 | 104.3065 | 9.5585  | 12.4575 | 1.9948 | 0.1766 | 0.1686 |
| BWMDR11 | 95.6716  | 17.5876 | 15.739  | 2.0713 | 0.2845 | 0.2505 |
| BWMDR12 | 105.0835 | 17.0459 | 16.1712 | 1.9495 | 0.3194 | 0.2875 |
| BWMVR12 | 108.0916 | 9.7028  | 15.6752 | 1.3842 | 0.3352 | 0.3166 |
| BWMVL12 | 111.732  | 10.0681 | 11.9005 | 1.6474 | 0.265  | 0.2634 |
| BWMDL12 | 109.9199 | 17.105  | 12.4998 | 2.0599 | 0.3072 | 0.3218 |
| BWMDL13 | 117.713  | 17.2913 | 12.8781 | 1.5781 | 0.31   | 0.3854 |
| BWMDR13 | 112.1239 | 17.3636 | 15.6619 | 1.7476 | 0.3059 | 0.2123 |
| BWMVL13 | 117.2876 | 9.7714  | 12.4879 | 1.2968 | 0.233  | 0.3638 |
| BWMVR13 | 113.577  | 9.5847  | 15.4863 | 2.3848 | 0.3229 | 0.3228 |
| BWMVR14 | 123.1617 | 9.9944  | 15.6033 | 1.7864 | 0.2798 | 0.2717 |
| BWMDR14 | 119.935  | 16.9269 | 16.0974 | 2.3703 | 0.2084 | 0.3514 |
| BWMDL14 | 126.4921 | 17.1815 | 12.6207 | 1.7279 | 0.2765 | 0.2768 |
| BWMVL14 | 126.8595 | 10.3506 | 12.0316 | 2.0913 | 0.2958 | 0.325  |
| BWMVR15 | 130.382  | 10.2806 | 15.2148 | 1.404  | 0.3016 | 0.2404 |
| BWMVL15 | 134.514  | 10.4058 | 12.449  | 1.258  | 0.3118 | 0.3218 |
| BWMVL16 | 148.1605 | 10.8328 | 12.1905 | 1.3353 | 0.2919 | 0.258  |
| BWMVR16 | 143.9198 | 10.6261 | 15.2238 | 1.3894 | 0.2671 | 0.2747 |
| BWMDR17 | 126.7395 | 17.2809 | 15.5262 | 2.0331 | 0.1871 | 0.3324 |
| BWMDL17 | 132.9749 | 17.2959 | 12.795  | 1.4415 | 0.2781 | 0.2806 |
| BWMDL18 | 145.0989 | 17.0904 | 12.4739 | 1.942  | 0.3297 | 0.364  |
| BWMDR18 | 138.4478 | 16.9694 | 15.6425 | 1.9267 | 0.3389 | 0.3411 |
| BWMDR19 | 148.9495 | 16.6608 | 15.3521 | 1.6159 | 0.5455 | 0.3805 |
| BWMDL19 | 155.7054 | 16.8827 | 12.7949 | 2.4452 | 0.3586 | 0.2928 |
| BWMVR19 | 154.2193 | 10.714  | 14.8952 | 1.2752 | 0.3359 | 0.2957 |
| BWMDR20 | 157.8237 | 16.5761 | 15.0778 | 1.2683 | 0.277  | 0.4094 |
| BWMDL20 | 167.4923 | 16.633  | 12.8257 | 1.5266 | 0.4966 | 0.3757 |
| BWMVL20 | 165.5066 | 10.9617 | 12.5016 | 1.3726 | 0.4694 | 0.4804 |

|         |          |         |         |        |        |        |
|---------|----------|---------|---------|--------|--------|--------|
| BWMVR20 | 164.6989 | 10.8039 | 14.9649 | 2.6799 | 0.3766 | 0.3474 |
| BWMDR22 | 169.4314 | 16.4528 | 15.2848 | 1.5459 | 0.2627 | 0.447  |
| BWMVL22 | 178.0113 | 11.3199 | 12.4715 | 2.1055 | 0.3596 | 0.5084 |
| BWMDL22 | 174.5994 | 16.6434 | 13.1308 | 1.3382 | 0.3394 | 0.3475 |
| BWMVR22 | 178.2483 | 11.2068 | 14.8141 | 1.367  | 0.2245 | 0.3999 |
| BWMVL23 | 200.4987 | 12.5384 | 12.844  | 1.3373 | 0.34   | 0.3881 |
| BWMDR23 | 178.6508 | 16.3842 | 15.0785 | 1.8846 | 0.3157 | 0.4179 |
| BWMDL23 | 183.4375 | 16.4759 | 12.9605 | 3.2878 | 0.338  | 0.3807 |
| BWMVR24 | 200.2523 | 12.2432 | 14.356  | 0.9359 | 0.3603 | 0.3322 |
| BWMDR24 | 199.0303 | 15.41   | 14.0412 | 1.0666 | 0.3215 | 0.4261 |
| BWMDL24 | 202.5051 | 15.7003 | 14.0449 | 0.8314 | 0.2113 | 0.4027 |
| DEP     | 192.9262 | 16.2198 | 14.8919 | 2.2637 | 0.2931 | 0.4603 |
| IML     | 185.134  | 12.2431 | 12.2853 | 2.9502 | 1.0417 | 0.4412 |
| IMR     | 184.0541 | 11.8148 | 15.4691 | 1.6999 | 0.4898 | 0.3148 |
| SPH     | 188.5045 | 13.271  | 12.1695 | 1.0123 | 0.387  | 0.228  |
| M       | 159.3569 | 14.045  | 15.5295 | 1.4946 | 0.3763 | 0.3115 |
| CCL1    | 128.3318 | 10.5849 | 12.2128 | 4.5246 | 0.3762 | 0.7837 |
| CCR1    | 100.2681 | 10.1209 | 16.0302 | 1.9658 | 0.228  | 0.3879 |
| CCR2    | 103.5954 | 10.0272 | 15.7808 | 1.5213 | 0.2949 | 0.3922 |
| CCL2    | 133.5711 | 10.9736 | 11.8213 | 4.4208 | 0.594  | 0.4556 |
| Z1      | 134.3546 | 11.2027 | 15.0856 | 1.5989 | 0.4311 | 0.3147 |
| Z2      | 137.7753 | 11.9338 | 14.482  | 1.8288 | 0.3784 | 0.6235 |
| Z4      | 144.7542 | 11.3387 | 12.6331 | 1.3832 | 0.3632 | 0.2557 |
| Z3      | 141.5134 | 11.7045 | 12.9273 | 1.3549 | 0.3771 | 0.1823 |
| INVR1   | 90.7634  | 11.2179 | 15.2915 | 2.0557 | 0.2283 | 0.2914 |
| INDR1   | 91.3765  | 15.9921 | 15.7089 | 1.6602 | 0.3959 | 0.3241 |
| INDL1   | 91.9531  | 15.8599 | 12.8395 | 1.7662 | 0.4163 | 0.3602 |
| INVL1   | 90.7217  | 10.8506 | 12.5826 | 2.0757 | 0.3517 | 0.2333 |
| INV3    | 99.1568  | 10.9034 | 13.4836 | 1.9613 | 0.2744 | 0.3759 |
| IND3    | 99.3984  | 16.0312 | 14.5523 | 1.6236 | 0.2075 | 0.5668 |
| INV4    | 109.5017 | 11.1436 | 13.8663 | 2.3381 | 0.2594 | 0.3337 |
| IND4    | 108.2125 | 15.9679 | 13.96   | 2.0287 | 0.3913 | 0.4159 |
| IND5    | 118.2131 | 15.5977 | 13.9276 | 2.0686 | 0.1778 | 0.2887 |
| INV5    | 122.3827 | 11.1678 | 13.875  | 2.2013 | 0.4127 | 0.3164 |
| INV6    | 136.05   | 14.0287 | 12.7947 | 3.0357 | 0.7988 | 0.618  |
| IND6    | 129.3993 | 15.4795 | 14.6477 | 1.6876 | 0.7763 | 0.4211 |

|                  |          |         |         |         |        |        |
|------------------|----------|---------|---------|---------|--------|--------|
| IND7             | 150.9741 | 15.3234 | 13.263  | 1.7453  | 0.4496 | 0.4106 |
| INV7             | 145.1131 | 13.6064 | 14.6319 | 2.4879  | 0.9307 | 0.4212 |
| INV8             | 159.237  | 11.9156 | 13.2802 | 2.188   | 0.2955 | 0.2661 |
| IND8             | 165.2543 | 15.3198 | 13.9953 | 1.5709  | 0.3825 | 0.3882 |
| IND9             | 177.745  | 15.4165 | 13.9261 | 0.9754  | 0.3475 | 0.364  |
| INV9             | 172.9927 | 12      | 13.9768 | 1.5104  | 0.217  | 0.5597 |
| INV10            | 183.9106 | 12.589  | 14.3137 | 0.9709  | 0.3942 | 0.4488 |
| IND10            | 185.5297 | 15.5155 | 12.9633 | 0.9509  | 0.4176 | 0.374  |
| BDUR             | 96.6113  | 12.8217 | 16.6419 | 1.5577  | 0.4566 | 0.4472 |
| BDUL             | 95.3364  | 13.2058 | 11.405  | 2.0141  | 0.6441 | 0.2946 |
| ALML             | 120.005  | 16.09   | 11.7588 | 4.5872  | 0.4088 | 0.3251 |
| ALMR             | 119.0367 | 15.8699 | 16.4671 | 6.1899  | 0.3473 | 0.2718 |
| CANR             | 132.1686 | 13.4887 | 16.5022 | 2.7972  | 0.4493 | 0.3202 |
| CANL             | 136.2313 | 13.766  | 11.024  | 2.5909  | 0.7123 | 0.2463 |
| HSNL             | 146.5365 | 12.44   | 11.078  | 11.3745 | 0.658  | 0.2039 |
| HSNR             | 143.6904 | 11.609  | 16.1299 | 4.151   | 0.5661 | 0.376  |
| hyp3.ABPLAAPAAAA | 23.7009  | 16.0014 | 14.2141 | 1.6098  | 0.3308 | 0.4197 |
| hyp3.ABPRAAPAAAA | 26.288   | 16.0517 | 14.1686 | 1.6424  | 0.3022 | 0.4475 |
| hyp4.ABARPAPAPA  | 16.6737  | 15.0357 | 14.1938 | 2.6469  | 0.4117 | 0.5034 |
| hyp4.ABPLAAPPAA  | 16.9571  | 10.1833 | 14.178  | 2.6163  | 0.4397 | 0.4452 |
| hyp4.ABPRAAPPAA  | 20.7696  | 9.7666  | 14.2918 | 2.2078  | 0.2188 | 0.3618 |
| hyp5.ABARPAPPAP  | 25.4284  | 13.0219 | 16.9168 | 1.5889  | 0.449  | 0.2902 |
| hyp5.ABPLAAAPAP  | 24.9271  | 12.8136 | 11.6061 | 1.8288  | 0.555  | 0.2399 |
| hyp6.ABPLAAAAPA  | 31.6947  | 16.6501 | 14.3119 | 2.1872  | 0.2729 | 0.4901 |
| hyp6.ABARPAAPAA  | 36.7031  | 16.6868 | 14.3625 | 2.0062  | 0.4151 | 0.4084 |
| hyp6.ABPLAAAPP   | 42.569   | 17.0912 | 14.2801 | 2.5551  | 0.3468 | 0.2694 |
| hyp6.ABARPAPAPP  | 45.6965  | 17.0276 | 14.1534 | 1.7242  | 0.2922 | 0.4622 |
| hyp6.ABPLAAPPAP  | 32.1217  | 8.8456  | 14.023  | 2.697   | 0.4442 | 0.3619 |
| hyp6.ABPRAAPPAP  | 39.2078  | 8.7242  | 13.9465 | 3.173   | 0.2532 | 0.3272 |
| hyp7.ABARPAAPAP  | 50.2831  | 17.6117 | 14.1865 | 1.3915  | 0.4929 | 0.511  |
| hyp7.ABARPAAPPA  | 62.3261  | 18.027  | 14.2075 | 2.2661  | 0.4051 | 0.4435 |
| hyp7.ABPLAAPPPA  | 46.5866  | 8.3512  | 13.8492 | 2.9014  | 0.3614 | 0.3033 |
| hyp7.ABPRAAPPPA  | 51.4768  | 8.2588  | 13.8666 | 1.8599  | 0.2247 | 0.3437 |
| hyp7.ABARPPPAPA  | 87.8573  | 14.0701 | 10.7148 | 2.7945  | 0.7818 | 0.3059 |
| hyp7.ABARPPAAPA  | 86.4489  | 13.3976 | 17.4711 | 3.1668  | 1.114  | 0.3944 |
| hyp7.ABARPAAPPP  | 89.601   | 13.2878 | 16.462  | 2.922   | 1.1017 | 2.0417 |

|                 |          |         |         |        |        |        |
|-----------------|----------|---------|---------|--------|--------|--------|
| hyp7.ABPLAAPP   | 90.2054  | 12.7991 | 10.8195 | 2.2157 | 0.7477 | 0.3065 |
| hyp7.ABPRAAPP   | 91.9882  | 13.4647 | 17.2944 | 2.9339 | 0.7819 | 0.3633 |
| hyp7.CAAAAAA    | 101.5401 | 14.933  | 10.9567 | 4.5724 | 0.3619 | 0.3491 |
| hyp7.CPAAAAA    | 103.9471 | 14.6053 | 16.9152 | 3.7808 | 0.4881 | 1.3954 |
| hyp7.CPAAAP     | 118.644  | 14.3452 | 17.1311 | 4.0184 | 0.4359 | 0.2924 |
| hyp7.CAAAAP     | 116.8091 | 14.8404 | 11.0613 | 5.0857 | 0.5061 | 0.2446 |
| hyp7.CPAAPA     | 134.8953 | 14.675  | 16.8859 | 2.9867 | 0.6299 | 0.414  |
| hyp7.CAAAPA     | 132.4916 | 15.2353 | 11.123  | 2.1586 | 0.4152 | 0.3234 |
| hyp7.CAAAPP     | 152.7025 | 14.7835 | 11.1285 | 4.3837 | 0.5974 | 0.2332 |
| hyp7.CPAAPP     | 153.1603 | 14.6572 | 16.5101 | 1.3893 | 0.5596 | 0.3772 |
| hyp7.CPAPAA     | 170.5995 | 15.2925 | 11.6329 | 2.3233 | 0.5658 | 0.2291 |
| hyp7.CPAPAP     | 172.3742 | 14.6608 | 15.9696 | 1.9226 | 0.4182 | 1.1713 |
| hyp7.CAAPPD     | 192.8562 | 15.0669 | 16.125  | 3.508  | 0.5592 | 0.4424 |
| hyp7.CPAPPD     | 191.6516 | 15.6912 | 11.9014 | 2.5178 | 0.4671 | 0.3746 |
| hyp7.ABPLAPP    | 205.6218 | 12.7451 | 13.7412 | 1.3993 | 0.4852 | 0.4689 |
| hyp7.ABPRAPP    | 208.2641 | 12.7282 | 13.7118 | 1.3819 | 0.4878 | 0.2586 |
| hyp8.ABPLPPPAP  | 212.766  | 13.2688 | 13.9047 | 1.5003 | 0.6231 | 0.328  |
| hyp9.ABPRPPAP   | 216.6096 | 13.8156 | 13.7962 | 1.5739 | 0.5    | 0.1826 |
| hyp10.ABPLPPPP  | 219.2666 | 14.2346 | 13.74   | 1.6552 | 0.2983 | 0.2756 |
| hyp10.ABPRPPPPP | 221.9663 | 14.4202 | 13.7403 | 2.2579 | 0.5295 | 0.3151 |
| hyp11.CPAPPV    | 212.5806 | 14.363  | 13.3943 | 1.6649 | 0.8181 | 0.3661 |
| EXC             | 69.3254  | 10.4155 | 13.4116 | 1.3657 | 0.4605 | 0.8755 |
| AVG             | 77.1979  | 8.572   | 13.9266 | 1.9227 | 0.3566 | 0.3885 |
| SABD            | 77.6226  | 9.1012  | 14.8454 | 2.2417 | 0.4135 | 0.5226 |
| SABVL           | 72.9957  | 8.5568  | 13.376  | 1.486  | 0.4899 | 0.4392 |
| SABVR           | 72.9075  | 8.7625  | 14.3405 | 1.9806 | 0.3265 | 0.324  |
| RIGL            | 77.732   | 8.8487  | 13.0691 | 2.1817 | 0.2685 | 0.2444 |
| RIGR            | 82.4366  | 8.7771  | 13.5354 | 2.0963 | 0.4092 | 0.4233 |
| RIFL            | 75.1103  | 8.9291  | 13.2219 | 1.7332 | 0.404  | 0.432  |
| RIFR            | 74.7236  | 8.9941  | 14.4948 | 1.9516 | 0.4684 | 0.4133 |
| DD1             | 80.0885  | 8.915   | 13.369  | 2.3948 | 0.4508 | 0.3549 |
| DD2             | 101.8    | 9.0119  | 13.8591 | 1.7764 | 0.2339 | 0.2702 |
| DD3             | 125.2717 | 9.3077  | 13.435  | 1.6072 | 0.2489 | 0.2929 |
| DD4             | 149.0062 | 9.8452  | 13.3149 | 1.4418 | 0.3008 | 0.3646 |
| DD5             | 169.8986 | 10.3389 | 13.42   | 0.9445 | 0.2045 | 0.4841 |
| DD6             | 189.2695 | 12.2519 | 13.5138 | 1.1397 | 0.3753 | 0.4355 |

|       |          |         |         |        |        |        |
|-------|----------|---------|---------|--------|--------|--------|
| DA1   | 84.5648  | 8.8786  | 13.7365 | 1.8004 | 0.3339 | 0.1904 |
| DA2   | 94.8159  | 8.9337  | 13.658  | 1.8025 | 0.2529 | 0.2518 |
| DA3   | 107.5526 | 8.8943  | 13.7482 | 1.7565 | 0.2703 | 0.2667 |
| DA4   | 122.2212 | 9.1585  | 13.5184 | 1.7939 | 0.2125 | 0.301  |
| DA5   | 139.315  | 9.5018  | 13.5157 | 2.6798 | 0.2727 | 0.3253 |
| DA6   | 159.9205 | 10.0273 | 13.4106 | 1.3188 | 0.3375 | 0.4007 |
| DA7   | 177.3755 | 10.6037 | 13.3695 | 1.2034 | 0.251  | 0.4676 |
| DA8   | 190.3654 | 11.5681 | 12.877  | 1.1362 | 0.3445 | 0.4414 |
| DA9   | 191.1491 | 11.8151 | 14.4859 | 1.0509 | 0.3952 | 0.443  |
| DB1   | 79.9446  | 8.5452  | 14.2018 | 1.7327 | 0.471  | 0.5791 |
| DB2   | 70.9565  | 8.3695  | 13.7465 | 1.7019 | 0.4004 | 0.515  |
| DB3   | 91.2527  | 8.8748  | 13.78   | 1.8673 | 0.2969 | 0.2102 |
| DB4   | 111.9606 | 8.937   | 13.5096 | 1.2902 | 0.1916 | 0.2807 |
| DB5   | 132.9304 | 9.5754  | 13.5212 | 1.3741 | 0.3072 | 0.2764 |
| DB6   | 155.9459 | 9.9611  | 13.2815 | 1.1109 | 0.3372 | 0.4391 |
| DB7   | 173.9199 | 10.4917 | 13.4488 | 1.2419 | 0.1822 | 0.4963 |
| PVT   | 186.5875 | 11.5147 | 14.1278 | 1.138  | 0.2944 | 0.408  |
| PVPL  | 187.4885 | 11.9692 | 12.6069 | 1.5126 | 0.6319 | 0.2198 |
| PVPR  | 188.4491 | 11.9385 | 14.8048 | 1.277  | 0.4352 | 0.2933 |
| PVQL  | 193.6694 | 13.8411 | 12.0361 | 0.8593 | 0.664  | 0.423  |
| PVQR  | 193.899  | 13.035  | 15.5114 | 0.9488 | 0.4523 | 0.3065 |
| virL  | 189.3212 | 15.0815 | 13.2298 | 1.0817 | 0.3563 | 0.2563 |
| virR  | 189.4832 | 14.4068 | 14.8201 | 1.0568 | 0.4436 | 0.3001 |
| PHAL  | 195.6076 | 13.1918 | 12.3061 | 0.781  | 0.5606 | 0.2416 |
| PHAR  | 195.804  | 12.544  | 15.05   | 0.8345 | 0.6425 | 0.2189 |
| PHBL  | 195.6812 | 14.6467 | 12.3637 | 0.8262 | 0.5882 | 0.2541 |
| PHBR  | 196.0306 | 13.9382 | 15.4962 | 0.9961 | 0.5722 | 0.3254 |
| LUAL  | 197.446  | 14.8396 | 12.5286 | 0.7665 | 0.8086 | 0.2937 |
| LUAR  | 197.49   | 14.1651 | 15.3239 | 0.9738 | 0.7707 | 0.3628 |
| PVCL  | 198.7062 | 13.8709 | 12.5081 | 1.0938 | 0.3409 | 0.2212 |
| PVCR  | 198.8902 | 13.3855 | 15.0883 | 1.3996 | 0.4684 | 0.2789 |
| ALNL  | 199.7526 | 15.4365 | 12.8839 | 1.0335 | 0.2886 | 0.3649 |
| ALNR  | 200.0039 | 14.9724 | 15.0448 | 0.8793 | 0.3691 | 0.4527 |
| PHshL | 201.4279 | 14.2546 | 13.0187 | 1.0931 | 0.2755 | 0.3696 |
| PHshR | 201.4972 | 14.089  | 14.5276 | 1.2618 | 0.5834 | 0.664  |
| PLML  | 205.2378 | 13.7289 | 13.0966 | 3.0586 | 0.9307 | 0.341  |

|        |          |         |         |        |        |        |
|--------|----------|---------|---------|--------|--------|--------|
| PLMR   | 204.6093 | 13.5378 | 14.3418 | 3.0165 | 0.6739 | 0.3975 |
| PVR    | 207.7403 | 14.5807 | 14.1786 | 2.6687 | 0.4383 | 0.4997 |
| DVA    | 196.3306 | 15.2158 | 14.0217 | 1.1188 | 0.3391 | 0.5809 |
| DVC    | 199.1947 | 13.9973 | 13.8202 | 1.916  | 0.5892 | 0.3195 |
| Y_PDA  | 193.4548 | 11.0699 | 13.4414 | 1.4571 | 0.2405 | 0.3773 |
| U      | 192.0989 | 12.6073 | 13.1611 | 0.9819 | 0.3321 | 0.3515 |
| B      | 197.2684 | 12.7229 | 13.6117 | 1.15   | 0.5459 | 0.2062 |
| F      | 194.6503 | 14.1519 | 13.8153 | 0.8775 | 0.3031 | 0.2243 |
| K      | 193.7243 | 15.5455 | 13.2958 | 0.9098 | 0.4751 | 0.7046 |
| K'     | 193.2935 | 14.785  | 15.1901 | 0.8943 | 0.3853 | 0.5105 |
| repD   | 192.5529 | 15.8318 | 13.9741 | 1.1573 | 0.6722 | 0.7353 |
| repVL  | 190.9468 | 13.6016 | 12.1921 | 0.9427 | 0.6165 | 0.2455 |
| repVR  | 191.0073 | 13.2314 | 15.5941 | 0.8229 | 0.6244 | 0.2926 |
| TL     | 205.8127 | 14.5202 | 13.2754 | 1.0589 | 0.4268 | 0.512  |
| TR     | 205.6555 | 14.3542 | 14.5702 | 1.2362 | 0.3855 | 0.4896 |
| pm1DL  | 41.5893  | 14.8485 | 14.0804 | 1.6107 | 0.3747 | 0.5437 |
| pm1DR  | 41.4313  | 14.7858 | 14.8629 | 1.1925 | 0.3683 | 0.6767 |
| pm1L   | 40.9535  | 12.6978 | 12.4973 | 1.4174 | 0.5419 | 0.3239 |
| pm1VL  | 41.0545  | 11.1977 | 12.9004 | 1.5899 | 0.468  | 0.3707 |
| pm1R   | 40.7154  | 12.5461 | 15.8894 | 1.2446 | 0.5626 | 0.2272 |
| pm1VR  | 40.8782  | 11.0666 | 15.1474 | 1.4515 | 0.5181 | 0.3531 |
| pm2D1  | 26.6143  | 14.669  | 14.2634 | 2.0798 | 0.2124 | 0.2823 |
| pm2D2  | 28.7944  | 14.773  | 14.2933 | 2.0586 | 0.2529 | 0.1545 |
| pm2VL1 | 25.5645  | 11.4653 | 12.946  | 2.2835 | 0.3338 | 0.257  |
| pm2VL2 | 27.7375  | 11.4481 | 12.8137 | 2.1362 | 0.2831 | 0.2502 |
| pm2VR1 | 25.4907  | 11.6363 | 15.6559 | 2.2236 | 0.3267 | 0.3237 |
| pm2VR2 | 27.8554  | 11.578  | 15.5977 | 1.7336 | 0.3303 | 0.3035 |
| pm3DL  | 31.904   | 14.3688 | 13.6248 | 1.2715 | 0.3692 | 0.2935 |
| pm3DR  | 34.4456  | 14.3914 | 14.8349 | 1.3026 | 0.4481 | 0.3161 |
| pm3L   | 36.2824  | 12.5524 | 12.6349 | 1.7027 | 0.4068 | 0.3326 |
| pm3VL  | 31.7293  | 11.1771 | 13.1842 | 1.1011 | 0.3865 | 0.3313 |
| pm3R   | 35.8362  | 12.4426 | 15.6671 | 1.4    | 0.3771 | 0.3423 |
| pm3VR  | 31.5689  | 11.141  | 14.9601 | 1.5973 | 0.4176 | 0.4199 |
| pm4DL  | 44.3583  | 15.1014 | 13.2792 | 1.5422 | 0.343  | 0.2974 |
| pm4DR  | 44.3422  | 15.0911 | 15.3902 | 1.2252 | 0.2648 | 0.2609 |
| pm4L   | 43.9716  | 13.0817 | 11.9365 | 1.5269 | 0.4505 | 0.4335 |

|        |         |         |         |        |        |        |
|--------|---------|---------|---------|--------|--------|--------|
| pm4VL  | 43.7656 | 10.3525 | 13.0078 | 1.5532 | 0.3627 | 0.3053 |
| pm4R   | 43.9142 | 12.8624 | 16.2473 | 1.3783 | 0.3703 | 0.1932 |
| pm4VR  | 43.7973 | 10.301  | 14.9811 | 1.4978 | 0.2958 | 0.2963 |
| pm5DL  | 71.8223 | 15.3824 | 13.4769 | 1.6239 | 0.5006 | 0.2608 |
| pm5DR  | 71.8333 | 15.5067 | 14.9348 | 1.7855 | 0.5442 | 0.3186 |
| pm5L   | 71.8567 | 13.5737 | 12.6825 | 1.9621 | 0.3541 | 0.2603 |
| pm5VL  | 72.5179 | 11.7271 | 13.5513 | 1.9588 | 0.3322 | 0.2605 |
| pm5R   | 71.6505 | 13.7614 | 15.7073 | 1.8204 | 0.5979 | 0.2497 |
| pm5VR  | 72.5345 | 11.7448 | 14.8193 | 2.0237 | 0.3755 | 0.2211 |
| pm6D   | 75.5933 | 16.2688 | 14.3106 | 1.6949 | 0.3753 | 0.3007 |
| pm6VL  | 75.4253 | 12.2651 | 12.5282 | 2.1763 | 0.2527 | 0.2214 |
| pm6VR  | 75.411  | 12.2616 | 15.8131 | 2.0262 | 0.3551 | 0.2372 |
| pm7D   | 78.5098 | 16.7498 | 14.2751 | 1.7168 | 0.2766 | 0.3316 |
| pm7VL  | 78.3769 | 12.219  | 12.0822 | 2.1032 | 0.3581 | 0.253  |
| pm7VR  | 78.498  | 12.1423 | 16.1027 | 2.173  | 0.3298 | 0.2393 |
| pm8    | 81.461  | 12.1285 | 14.0164 | 2.238  | 0.3977 | 0.3563 |
| mc1DL  | 41.6045 | 14.1653 | 12.8783 | 1.5206 | 0.4001 | 0.3181 |
| mc1DR  | 41.5389 | 14.0166 | 15.7923 | 1.318  | 0.4384 | 0.3091 |
| mc1V   | 41.4059 | 10.4537 | 14.0028 | 1.434  | 0.3871 | 0.3033 |
| mc2DL  | 69.8031 | 14.4008 | 13.204  | 1.9795 | 0.5182 | 0.2824 |
| mc2DR  | 69.3575 | 14.4065 | 15.1006 | 1.5399 | 0.6443 | 0.2333 |
| mc2V   | 69.6884 | 12.2413 | 14.1826 | 2.0009 | 0.3511 | 0.2339 |
| mc3DL  | 78.5951 | 14.6059 | 11.9222 | 1.9509 | 0.4901 | 0.2903 |
| mc3DR  | 78.7665 | 14.6905 | 16.5954 | 1.9378 | 0.2666 | 0.2393 |
| mc3V   | 78.4526 | 10.5774 | 14.2746 | 2.208  | 0.2021 | 0.3047 |
| vpi1   | 82.7389 | 16.2306 | 14.4741 | 1.9505 | 0.4511 | 0.5456 |
| vpi2DL | 82.6554 | 14.693  | 12.3631 | 1.9742 | 0.5686 | 0.5232 |
| vpi2DR | 82.8286 | 14.5672 | 15.9977 | 1.9675 | 0.3914 | 0.2876 |
| vpi2V  | 82.4441 | 11.4488 | 14.0642 | 2.2647 | 0.5912 | 0.5462 |
| vpi3D  | 83.9921 | 15.6925 | 14.1925 | 2.0144 | 0.5161 | 0.5729 |
| vpi3V  | 83.4732 | 11.9514 | 14.108  | 2.3408 | 0.4878 | 0.6262 |
| e1D    | 32.6375 | 14.8266 | 14.3126 | 1.794  | 0.3297 | 0.4972 |
| e1VL   | 30.7039 | 11.572  | 12.631  | 1.8763 | 0.3537 | 0.3433 |
| e1VR   | 30.8187 | 11.5889 | 15.6019 | 1.8342 | 0.4162 | 0.4191 |
| e2D    | 22.7671 | 14.6737 | 14.2737 | 2.2273 | 0.2564 | 0.267  |
| e2VL   | 21.8997 | 11.5289 | 13.0345 | 2.3651 | 0.2293 | 0.2284 |

|       |         |         |         |        |        |        |
|-------|---------|---------|---------|--------|--------|--------|
| e2VR  | 21.8028 | 11.6371 | 15.5801 | 2.3485 | 0.4298 | 0.3094 |
| e3D   | 37.8875 | 14.9201 | 14.4016 | 1.6212 | 0.2132 | 0.2585 |
| e3VL  | 34.3    | 11.4771 | 12.605  | 1.3556 | 0.3201 | 0.3135 |
| e3VR  | 34.7601 | 11.5717 | 15.6294 | 1.6809 | 0.4041 | 0.3948 |
| I1L   | 38.5515 | 11.897  | 12.8063 | 1.58   | 0.3504 | 0.3307 |
| I1R   | 38.4653 | 11.791  | 15.4774 | 1.5706 | 0.4591 | 0.2855 |
| I2L   | 43.0853 | 11.3372 | 11.93   | 1.7988 | 0.3011 | 0.2328 |
| I2R   | 43.0739 | 11.182  | 16.1489 | 1.533  | 0.3982 | 0.3744 |
| I3    | 45.8117 | 15.1384 | 14.2671 | 1.2781 | 0.2283 | 0.2673 |
| I4    | 73.3828 | 16.3462 | 14.2513 | 1.5404 | 0.3773 | 0.2986 |
| I5    | 74.2929 | 10.8755 | 14.099  | 2.0503 | 0.2762 | 0.308  |
| I6    | 75.6562 | 15.8863 | 12.577  | 1.6264 | 0.2945 | 0.3581 |
| MCL   | 42.9562 | 11.9662 | 12.9345 | 1.6374 | 0.3081 | 0.2438 |
| MCR   | 42.6822 | 11.8131 | 15.2755 | 1.6127 | 0.325  | 0.2945 |
| MI    | 44.0883 | 15.3836 | 14.3402 | 1.3018 | 0.2189 | 0.299  |
| NSML  | 45.4828 | 11.4604 | 12.3031 | 1.7052 | 0.3217 | 0.2116 |
| NSMR  | 45.5503 | 11.4047 | 15.725  | 1.5274 | 0.2852 | 0.2762 |
| M1    | 75.6296 | 15.7365 | 15.9563 | 1.4781 | 0.5883 | 0.2723 |
| M2L   | 73.2154 | 12.4379 | 12.5246 | 1.8924 | 0.3022 | 0.2022 |
| M2R   | 73.1784 | 12.6327 | 16.0257 | 1.8962 | 0.4178 | 0.361  |
| M3L   | 49.0567 | 11.8658 | 12.8971 | 1.8276 | 0.2031 | 0.2432 |
| M3R   | 49.1127 | 11.8307 | 15.2438 | 1.5887 | 0.3125 | 0.1552 |
| M4    | 49.203  | 14.2718 | 14.1635 | 1.5231 | 0.232  | 0.1578 |
| M5    | 79.1804 | 15.8854 | 12.6419 | 1.7568 | 0.4173 | 0.3306 |
| g1AL  | 74.0577 | 14.7402 | 12.3568 | 1.7322 | 0.5017 | 0.3771 |
| g1AR  | 73.9558 | 14.9566 | 16.1186 | 1.6977 | 0.4639 | 0.3496 |
| g1P   | 80.6074 | 15.6935 | 15.5454 | 1.9336 | 0.3137 | 0.3272 |
| g2L   | 80.3949 | 11.4191 | 12.9506 | 2.3046 | 0.3278 | 0.333  |
| g2R   | 80.5197 | 11.4916 | 15.1513 | 2.2119 | 0.2886 | 0.3113 |
| G1    | 61.4851 | 8.405   | 13.7388 | 1.0063 | 0.2426 | 0.2491 |
| G2    | 64.7539 | 9.035   | 13.8511 | 1.0624 | 0.424  | 0.2799 |
| W     | 68.2584 | 8.5828  | 13.4221 | 1.843  | 0.3661 | 0.4197 |
| ARCAV | 24.4012 | 9.5986  | 14.1883 | 2.0176 | 0.2991 | 0.4617 |
| ARCAL | 31.3776 | 12.9039 | 11.3492 | 1.9568 | 0.6287 | 0.3315 |
| ARCAR | 32.1269 | 12.8881 | 17.1083 | 1.3986 | 0.7831 | 0.239  |

```

# Note:
# In the following we display three columns, the first is the most commonly used
# cell/nuclei names in literature, the second column is the lineage name, and the
# column is the cell names used in this paper. In many cases, the cell names in the
# third column are easier to understand for a non-worm-biologist; however, we provide
# all three so that one can easily convert one to another. These three names for any
# cell are also incorporated in the .apo digital atlas file, which is another Supplementary
# file for this paper. The digital atlas file is a common CSV file (comma separated value)
# and can be opened using V3D (http://penglab.janelia.org) or other text/spreadsheet editors
# (e.g. Excel).
#
# Also note that in the following, if in a row there is no respective name in the third column,
# that means the cell name used in this paper is the same to the conventional name.
#

```

| conventional cell name | cell lineage name | cell name used in this paper |
|------------------------|-------------------|------------------------------|
| INT1DL                 | EALAAD            | INDL1                        |
| INT1VL                 | EALAAV            | INVL1                        |
| INT1DR                 | EARAAD            | INDR1                        |
| INT1VR                 | EARAAV            | INVR1                        |
| INT2V                  | EALPA             | INV3                         |
| INT2D                  | EARPA             | IND3                         |
| INT3V                  | EALAP             | INV4                         |
| INT3D                  | EARAP             | IND4                         |
| INT4V                  | EPLAA             | INV5                         |
| INT4D                  | EPRAA             | IND5                         |
| INT5L                  | EALPP             | INV6                         |
| INT5R                  | EARPP             | IND6                         |
| INT6L                  | EPLAP             | IND7                         |
| INT6R                  | EPRAP             | INV7                         |
| INT7L                  | EPLPA             | IND8                         |
| INT7R                  | EPRPA             | INV8                         |
| INT8L                  | EPLPPA            | IND9                         |
| INT8R                  | EPRPPA            | INV9                         |
| INT9L                  | EPLPPP            | IND10                        |
| INT9R                  | EPRPPP            | INV10                        |

|            |           |        |
|------------|-----------|--------|
| MU_BODVL2  | MSAPPAPP  | BWMVL1 |
| MU_BODVR2  | MSPPPAPP  | BWMVR1 |
| MU_BODDL2  | MSAPAPPA  | BWMDL1 |
| MU_BODDR2  | MSPPAPPA  | BWMDR1 |
| MU_BODVL1  | MSAPAPAP  | BWMVL2 |
| MU_BODVR1  | MSPPAPAP  | BWMVR2 |
| MU_BODDL1  | MSAPAAAP  | BWMDL2 |
| MU_BODDR1  | MSPPAAAP  | BWMDR2 |
| MU_BODVL4  | DAAPA     | BWMVL3 |
| MU_BODVR4  | DPAPA     | BWMVR3 |
| MU_BODDL4  | MSAPPPPA  | BWMDL3 |
| MU_BODDR4  | MSPPPPPA  | BWMDR3 |
| MU_BODVL3  | MSAPPAA   | BWMVL4 |
| MU_BODVR3  | MSPPPPAA  | BWMVR4 |
| MU_BODDL3  | MSAPAPPP  | BWMDL4 |
| MU_BODDR3  | MSPPAPPP  | BWMDR4 |
| MU_BODVL6  | DAAPP     | BWMVL5 |
| MU_BODVR6  | DPAPP     | BWMVR5 |
| MU_BODDL6  | MSAPPPPP  | BWMDL5 |
| MU_BODDR6  | MSPPPPPP  | BWMDR5 |
| MU_BODVL5  | DAAAAA    | BWMVL6 |
| MU_BODVR5  | DPAAA     | BWMVR6 |
| MU_BODDL5  | MSAPPPAP  | BWMDL6 |
| MU_BODDR5  | MSPPPPAP  | BWMDR6 |
| MU_BODVL8  | MSAAPPAA  | BWMVL7 |
| MU_BODVR8  | MSPAPPPAA | BWMVR7 |
| MU_BODDL8  | DAPPAA    | BWMDL7 |
| MU_BODDR8  | DPPPAA    | BWMDR7 |
| MU_BODVL7  | DAPAA     | BWMVL8 |
| MU_BODVR7  | DPPAA     | BWMVR8 |
| MU_BODDL7  | DAAAP     | BWMDL8 |
| MU_BODDR7  | DPAAP     | BWMDR8 |
| MU_BODVL10 | MSAAPPAP  | BWMVL9 |
| MU_BODVR10 | MSPAPPPAP | BWMVR9 |
| MU_BODDL10 | DAPPAP    | BWMDL9 |
| MU_BODDR10 | DPPPAP    | BWMDR9 |

|            |           |         |
|------------|-----------|---------|
| MU_BODVL9  | CAPAAAA   | BWMVL10 |
| MU_BODVR9  | CPPAAAA   | BWMVR10 |
| MU_BODDL9  | DAPAP     | BWMDL10 |
| MU_BODDR9  | DPPAP     | BWMDR10 |
| MU_BODVL12 | MSAAPPPA  | BWMVL11 |
| MU_BODVR12 | MSPAPPPP  | BWMVR11 |
| MU_BODDL12 | DAPPPA    | BWMDL11 |
| MU_BODDR12 | DPPPA     | BWMDR11 |
| MU_BODVL11 | CAPAAAP   | BWMVL12 |
| MU_BODVR11 | CPPAAAP   | BWMVR12 |
| MU_BODDL11 | CAPPAAA   | BWMDL12 |
| MU_BODDR11 | CPPPAAA   | BWMDR12 |
| MU_BODVL14 | MSAAPPPP  | BWMVL13 |
| MU_BODVR14 | MSPAPPPP  | BWMVR13 |
| MU_BODDL14 | DAPPPP    | BWMDL13 |
| MU_BODDR14 | DPPPP     | BWMDR13 |
| MU_BODVL13 | CAPAAPA   | BWMVL14 |
| MU_BODVR13 | CPAAAPA   | BWMVR14 |
| MU_BODDL13 | CAPAPAA   | BWMDL14 |
| MU_BODDR13 | CPPAPAA   | BWMDR14 |
| MU_BODVL16 | MSPAPPAA  | BWMVL15 |
| MU_BODVR16 | MSPAPPAP  | BWMVR15 |
| MU_BODVL15 | CAPAAPP   | BWMVL16 |
| MU_BODVR15 | CPAAAPP   | BWMVR16 |
| MU_BODDL18 | CAPPAAP   | BWMDL17 |
| MU_BODDR18 | CPPPAAP   | BWMDR17 |
| MU_BODDL17 | CAPAPAP   | BWMDL18 |
| MU_BODDR17 | CPPAPAP   | BWMDR18 |
| MU_BODVR20 | ABPRPPPPA | BWMVR19 |
| MU_BODDL20 | CAPPAA    | BWMDL19 |
| MU_BODDR20 | CPPPAA    | BWMDR19 |
| MU_BODVL20 | CAPAPPA   | BWMVL20 |
| MU_BODVR19 | CPPAPPA   | BWMVR20 |
| MU_BODDL19 | CAPPAPA   | BWMDL20 |
| MU_BODDR19 | CPPPAPA   | BWMDR20 |
| MU_BODVL22 | CAPAPPP   | BWMVL22 |

|            |                          |         |
|------------|--------------------------|---------|
| MU_BODVR22 | CPPAPPP                  | BWMVR22 |
| MU_BODDL22 | CAPPPAP                  | BWMDL22 |
| MU_BODDR22 | CPPPPAP                  | BWMDR22 |
| MU_BODVL23 | CAPPPPV                  | BWMVL23 |
| MU_BODDL24 | CAPPPPD                  | BWMDL23 |
| MU_BODDR24 | CPPPPPD                  | BWMDR23 |
| MU_BODVR24 | CPPPPPV                  | BWMVR24 |
| MU_BODDL23 | CAPPAPP                  | BWMDL24 |
| MU_BODDR23 | CPPPAPP                  | DEP     |
| MU_ANAL    | ABPLPPPPPAP              | BWMDR24 |
| MU_INT_L   | ABPLPPPPPAA              | IML     |
| MU_INT_R   | MSPPAAPP                 | IMR     |
| MU_SPH     | ABPRPPPPPAP              | SPH     |
| PM1DL      | ABARAAPAAAP              |         |
| PM1DR      | ABARAAPPAAP              |         |
| PM1L       | ABARAAAAAAAP             |         |
| PM1VL      | ABALPAAAAPA              |         |
| PM1R       | ABARAAAAAPP              |         |
| PM1VR      | ABARAPAAAPA              |         |
| PM2DL      | ABARAAPAAPA_ABARAAPPAPA  | PM2D1   |
| PM2DR      | ABARAAPPAPA_ABARAAPAAAPA | PM2D2   |
| PM2VL      | ABALPAAAAP_ABALPAAAPAA   | PM2VL1  |
| PM2L       | ABALPAAAPAA_ABALPAAAAP   | PM2VL2  |
| PM2VR      | ABARAPAAAAP_ABARAPAAAPAA | PM2VR1  |
| PM2R       | ABARAPAAPAA_ABARAPAAAAP  | PM2VR2  |
| PM3DL      | MSAAAPAAA                |         |
| PM3DR      | MSPAAAAAPA               |         |
| PM3L       | ABALPAAPAPP              |         |
| PM3VL      | ABALPAPPPP               |         |
| PM3R       | ABARAPAAAPPA             |         |
| PM3VR      | ABARAPAPPPP              |         |
| PM4DL      | MSAAAAAPP                |         |
| PM4DR      | MSPAAAAAPP               |         |
| PM4L       | MSAAAPAAP                |         |
| PM4VL      | MSAAPAAAA                |         |
| PM4R       | ABARAAAPAPP              |         |

|        |              |
|--------|--------------|
| PM4VR  | MSPAPAAAAA   |
| PM5DL  | MSAAAAPAP    |
| PM5DR  | MSPAAAPPA    |
| PM5L   | ABARAAPAPAP  |
| PM5VL  | MSAAPAAAP    |
| PM5R   | ABARAAPPPAP  |
| PM5VR  | MSPAPAAAP    |
| PM6D   | MSPAAAPPP    |
| PM6VL  | MSAAPAPPA    |
| PM6VR  | MSPAPAPPA    |
| PM7D   | MSAAAAPPP    |
| PM7VL  | MSAAPAAPP    |
| PM7VR  | MSPAPAAPP    |
| PM8    | MSAAAPAPP    |
| MC1DL  | ABALPAAPAPA  |
| MC1DR  | ABARAAAPAPA  |
| MC1V   | ABALPAPPPPA  |
| MC2DL  | ABARAAPPAAPP |
| MC2DR  | ABARAAPPAPP  |
| MC2V   | ABARAPAPPPA  |
| MC3DL  | MSAAAPAPA    |
| MC3DR  | MSPAAPAPA    |
| MC3V   | ABALPAPPAPP  |
| VPI1   | MSPAAAPAPP   |
| VPI2DL | MSAAPAPPP    |
| VPI2DR | MSPAPAPPP    |
| VPI2V  | MSAAPPAA     |
| VPI3D  | MSAAAPPP     |
| VPI3V  | MSAAPPAP     |
| G1AL   | MSAAPAAPAA   |
| G1AR   | MSPAPAAPAA   |
| G1P    | MSAAAAAPAP   |
| G2L    | MSAAPAPAA    |
| G2R    | MSPAPAPAA    |
| I1L    | ABALPAPPPAA  |
| I1R    | ABARAPAPPAA  |

|       |               |
|-------|---------------|
| I2L   | ABALPAPPAAPA  |
| I2R   | ABARAPAPAAAPA |
| I3    | MSAAAAAPAA    |
| I4    | MSAAAAPAA     |
| I5    | ABARAPAPAPP   |
| I6    | MSPAAAPAA     |
| MCL   | ABALPAAAPPP   |
| MCR   | ABARAPAAPPP   |
| MI    | ABARAAPPAAA   |
| NSML  | ABARAAPAPAAV  |
| NSMR  | ABARAAPPPAAV  |
| M1    | MSPAAPAAA     |
| M2L   | ABARAAPAPPA   |
| M2R   | ABARAAPPPPA   |
| M3L   | ABARAAPAPPP   |
| M3R   | ABARAAPPPPP   |
| M4    | MSPAAAAAA     |
| M5    | MSPAAPAP      |
| BDUR  | ABARPPPAPPP   |
| BDUL  | ABARPPAAPPP   |
| ALML  | ABARPPAAPPA   |
| ALMR  | ABARPPPAPPA   |
| CANR  | ABALAPPAPPA   |
| CANL  | ABALAPAAAPA   |
| HSNL  | ABPLAPPPAPPA  |
| HSNR  | ABPRAPPPAPPA  |
| AVG   | ABPRPAPPPAP   |
| SABD  | ABPLPPAPAAAP  |
| SABVL | ABPLPPAPAAAA  |
| SABVR | ABPRPPAPAAAA  |
| RIGL  | ABPLPPAPPA    |
| RIGR  | ABPRPPAPPA    |
| RIFL  | ABPLPPAPAAAP  |
| RIFR  | ABPRPPAPAAAP  |
| DD1   | ABPLPPAPPAP   |
| DD2   | ABPRPPAPPAP   |

|      |                         |
|------|-------------------------|
| DD3  | ABPLPPAPPPA             |
| DD4  | ABPRPPAPPPA             |
| DD5  | ABPLPPAPPPP             |
| DD6  | ABPRPPAPPPP             |
| DA1  | ABPRPPAPAAP             |
| DA2  | ABPLPPAPAPA             |
| DA3  | ABPRPPAPAPA             |
| DA4  | ABPLPPAPAPP             |
| DA5  | ABPRPPAPAPP             |
| DA6  | ABPLPPPAAAP             |
| DA7  | ABPRPPPAAAP             |
| DA8  | ABPRPAPAPPP             |
| DA9  | ABPLPPPAAAA             |
| DB1  | ABPLAAAAPP_ABPRPAAAAPP  |
| DB2  | ABARAPPAPPA             |
| DB3  | ABPRPAAAAPP_ABPLPAAAAPP |
| DB4  | ABPRPAPPAPP             |
| DB5  | ABPLPAPAPP              |
| DB6  | ABPLPPAAPP              |
| DB7  | ABPRPPAAPP              |
| PVT  | ABPLPAPPPA              |
| PVPL | ABPLPPPAAA              |
| PVPR | ABPRPPPAAA              |
| PVQL | ABPLAPPPAAA             |
| PVQR | ABPRAPPPAAA             |
| PHAL | ABPLPPPAAPP             |
| PHAR | ABPRPPPAAPP             |
| PHBL | ABPLAPPPAPPP            |
| PHBR | ABPRAPPPAPPP            |
| LUAL | ABPLPPPAAPAP            |
| LUAR | ABPRPPPAAPAP            |
| PVCL | ABPLPPPAAPAA            |
| PVCR | ABPRPPPAAPAA            |
| ALNL | ABPLAPAPPPPAP           |
| ALNR | ABPRAPAPPPPAP           |
| PLML | ABPLAPAPPPPAA           |

|                  |                         |                  |
|------------------|-------------------------|------------------|
| PLMR             | ABPRAPAPPPPAA           |                  |
| PVR              | CAAPPV                  |                  |
| DVA              | ABPRPPPAPP              |                  |
| DVC              | CAAPAA                  |                  |
| ARC_ANT_V        | ABALPAPAAPA             | ARCAV            |
| ARC_ANT_DL       | ABALPAAPPAA             | ARCAL            |
| ARC_ANT_DR       | ABARAAAPPPA             | ARCAR            |
| E1D              | ABARAAAAPAP             |                  |
| E1VL             | ABARAAAAAAA             |                  |
| E1VR             | ABARAAAAAPAA            |                  |
| E2V              | ABALPAPPAPA             | E2D              |
| E2DL             | ABALPAAPAAP             | E2VL             |
| E2DR             | ABARAAAPPAAP            | E2VR             |
| E3D              | ABARAAPAAAAA            |                  |
| E3VL             | ABALPAAAAAA             |                  |
| E3VR             | ABARAPAAAAAA            |                  |
| B                | ABPRPPPPAPA             |                  |
| F                | ABPLPPPPAPP             |                  |
| K                | ABPLPAPPAA              |                  |
| K'               | ABPLPAPPAP              |                  |
| U                | ABPLPPPPAPA             |                  |
| Y/PDA            | ABPRPPPPAAA             |                  |
| HYP3_ABPLAAPAAAA | ABPLAAPAAAA_ABPRAAPAAAA | HYP3 ABPLAAPAAAA |
| HYP3_ABPRAAPAAAA | ABPRAAPAAAA_ABPLAAPAAAA | HYP3 ABPRAAPAAAA |
| HYP4_ABARPAPAPA  | ABARPAPAPA              | HYP4 ABARPAPAPA  |
| HYP4_ABPLAAPPAA  | ABPLAAPPAA_ABPRAAPPAA   | HYP4 ABPLAAPPAA  |
| HYP4_ABPRAAPPAA  | ABPRAAPPAA_ABPLAAPPAA   | HYP4 ABPRAAPPAA  |
| HYP5_ABARPAPPAP  | ABARPAPPAP              | HYP5 ABARPAPPAP  |
| HYP5_ABPLAAAPAP  | ABPLAAAPAP              | HYP5 ABPLAAAPAP  |
| HYP6_ABPLAAAAPA  | ABPLAAAAPA              | HYP6 ABPLAAAAPA  |
| HYP6_ABARPAAPAA  | ABARPAAPAA              | HYP6 ABARPAAPAA  |
| HYP6_ABPLAAAAPP  | ABPLAAAAPP              | HYP6 ABPLAAAAPP  |
| HYP6_ABARPAPAPP  | ABARPAPAPP              | HYP6 ABARPAPAPP  |
| HYP6_ABPLAAPPAP  | ABPLAAPPAP_ABPRAAPPAP   | HYP6 ABPLAAPPAP  |
| HYP6_ABPRAAPPAP  | ABPRAAPPAP_ABPLAAPPAP   | HYP6 ABPRAAPPAP  |
| HYP7_ABARPAAPAP  | ABARPAAPAP              | HYP7 ABARPAAPAP  |

|                   |                        |                   |
|-------------------|------------------------|-------------------|
| HYP7_ABARPAAPPA   | ABARPAAPPA             | HYP7 ABARPAAPPA   |
| HYP7_ABPLAAPPPA   | ABPLAAPPPA_ABPRAAPPPA  | HYP7 ABPLAAPPPA   |
| HYP7_ABPRAAPPPA   | ABPRAAPPPA_ABPLAAPPPA  | HYP7 ABPRAAPPPA   |
| HYP7_ABARPPPAPA   | ABARPPPAPA             | HYP7 ABARPPPAPA   |
| HYP7_ABARPPAAPA   | ABARPPAAPA             | HYP7 ABARPPAAPA   |
| HYP7_ABARPAAPPP   | ABARPAAPPP             | HYP7 ABARPAAPPP   |
| HYP7_ABPLAAPPPP   | ABPLAAPPPP             | HYP7 ABPLAAPPPP   |
| HYP7_ABPRAAPPPP   | ABPRAAPPPP             | HYP7 ABPRAAPPPP   |
| HYP7_CAAAAAA      | CAAAAAA                | HYP7 CAAAAAA      |
| HYP7_CPAAAA       | CPAAAAA                | HYP7 CPAAAA       |
| HYP7_CPAAAP       | CPAAAP                 | HYP7 CPAAAP       |
| HYP7_CAAAAP       | CAAAAP                 | HYP7 CAAAAP       |
| HYP7_CPAAPA       | CPAAPA                 | HYP7 CPAAPA       |
| HYP7_CAAAPA       | CAAAPA                 | HYP7 CAAAPA       |
| HYP7_CAAAPP       | CAAAPP                 | HYP7 CAAAPP       |
| HYP7_CPAAPP       | CPAAPP                 | HYP7 CPAAPP       |
| HYP7_CPAPAA       | CPAPAA                 | HYP7 CPAPAA       |
| HYP7_CPAAPAP      | CPAPAP                 | HYP7 CPAPAP       |
| HYP7_CAAAPPD      | CAAPPD                 | HYP7 CAAPPD       |
| HYP7_CPAAPPD      | CPAPPD                 | HYP7 CPAPPD       |
| HYP7_ABPLAPPPP    | ABPLAPPPP_ABPRAPPPP    | HYP7 ABPLAPPPP    |
| HYP7_ABPRAPPPP    | ABPRAPPPP_ABPLAPPPP    | HYP7 ABPRAPPPP    |
| HYP8_ABPLPPPAPAP  | ABPLPPPAPAP            | HYP8 ABPLPPPAPAP  |
| HYP9_ABPRPPPAPAP  | ABPRPPPAPAP            | HYP9 ABPRPPPAPAP  |
| HYP10_ABPLPPPPPPP | ABPLPPPPPP_ABPRPPPPPPP | HYP10 ABPLPPPPPPP |
| HYP10_ABPRPPPPPPP | ABPRPPPPPP_ABPLPPPPPPP | HYP10 ABPRPPPPPPP |
| HYP11_CPAAPPV     | CPAPPV                 | HYP11 CPAPPV      |
| EXC               | ABPLPAPPAAP            |                   |
| VIRL              | ABPRPAPPPP             |                   |
| VIRR              | ABPRPAPPPP             |                   |
| AMSHL             | ABPLAAPAAP             |                   |
| AMSHR             | ABPRAAPAAP             |                   |
| PHSHL             | ABPLPPPAPAA            |                   |
| PHSHR             | ABPRPPPAPAA            |                   |
| ADESHL            | ABARPPAAAA             | EXC GL L          |
| ADESHR            | ABARPPAAAA             | EXC GL R          |

|         |             |
|---------|-------------|
| HOL     | ABPLAAAPPA  |
| HOR     | ABARPAPPPA  |
| H1L     | ABPLAAAPPP  |
| H1R     | ABARPAPPPP  |
| H2L     | ABARPPAAAP  |
| H2R     | ABARPPPAAP  |
| G1      | ABPRPAAAAPA |
| G2      | ABPLAPAAPA  |
| W       | ABPRAPAAPA  |
| P1/2L   | ABPLAPAAPP  |
| P1/2R   | ABPRAPAAPP  |
| P11/12L | ABPLAPAPPA  |
| P11/12R | ABPRAPAPPA  |
| P3/4L   | ABPLAPPAAA  |
| P3/4R   | ABPRAPPAAA  |
| P5/6L   | ABPLAPPAAP  |
| P5/6R   | ABPRAPPAAAP |
| P7/8L   | ABPLAPPAPP  |
| P7/8R   | ABPRAPPAPP  |
| P9/10L  | ABPLAPAPAP  |
| P9/10R  | ABPRAPAPAP  |
| QL      | ABPLAPAPAAA |
| QR      | ABPRAPAPAAA |
| V1L     | ABARPPAPAA  |
| V1R     | ABARPPPPAA  |
| V2L     | ABARPPAPAP  |
| V2R     | ABARPPPPAP  |
| V3L     | ABPLAPPAPA  |
| V3R     | ABPRAPPAPA  |
| V4L     | ABARPPAPPA  |
| V4R     | ABARPPPPPA  |
| V5L     | ABPLAPAPAAP |
| V5R     | ABPRAPAPAAP |
| V6L     | ABARPPAPPP  |
| V6R     | ABARPPPPPP  |
| TL      | ABPLAPPPPP  |

HOL  
HOR

|         |             |       |
|---------|-------------|-------|
| TR      | ABPRAPPPPP  |       |
| M       | MSAPAAP     |       |
| Z1      | MSPPPAAP    |       |
| Z4      | MSAPPAAP    |       |
| CCAL    | MSAPAPAAA   | CCL1  |
| CCAR    | MSPPAPAAAA  | CCR1  |
| CCPR    | MSPPAPAAAP  | CCR2  |
| CCPL    | MSAPAPAAAP  | CCL2  |
| RECT_D  | ABPLPAPPPPP | REPD  |
| RECT_VL | ABPLPPPAAP  | REPVL |
| RECT_VR | ABPRPPPPAAP | REPVR |
| Z2      | P4P         |       |
| Z3      | P4A         |       |

## **Supplementary Note: Additional Details of Methods**

### **1. Worm body backbone detection**

We developed two algorithms,  $BDB^+$  and  $BDB^-$ , to detect the backbone of worm body in 2D and 3D respectively, under different scenarios<sup>1</sup>. Usually auto-fluorescence makes the pixel intensities of the worm body region reliably higher than the image background. It may be even more visible when all Z-sections in a 3D image stack are summed up together and projected to 2D. Under this scenario, a clear boundary of a worm body in the image can be identified. We thus used a simpler algorithm  $BDB^+$  to detect the backbone. Otherwise, when the outer boundary of the worm is hard to detect precisely we used a more sophisticated algorithm  $BDB^-$  to detect backbone. For the 15 images we used to build the atlas, we used the  $BDB^+$  algorithm. Supplementary Figure 1 illustrates the  $BDB^+$  algorithm. The upper and middle panels of Supplementary Video 1 demonstrate a 3D image before and after 3D straightening.

### **2. Intensity filling of hollow-shaped nuclei**

Some cells have a large nucleolus which is unstained by the reagent DAPI and this gives the nucleus a hollowed-out shape. Such a pattern can easily be broken into pieces when we apply thresholding and watershed algorithm to segment nuclear region from the image background. Thus we first detected these hollow-shaped patterns and filled them using the pixels surrounding them (Supplementary Fig. 2b).

Let  $I$  be the preprocessed image after straightening and filtering. We thresholded the image at multiple intensity levels  $v$  ( $v \in [v_{min}, v_{max}]$ , where  $v_{min}$  is the lowest intensity level of a typical nucleus determined by  $\mu + 2\sigma$ , with  $\mu$  and  $\sigma$  being the mean and standard deviation of the intensity of image  $I$ ). A “hole” in the thresholded image  $T_v(I)$  is any connected component of background pixels for which all of their surrounding foreground pixels are in a single connected component. The set of all pixels in holes,  $o(T_v(I))$  can be found with a morphological “fill” operation in time linear in the number of pixels in  $I$ . We then took the union of all the holes found at each level, i.e:

$$H = \cup_v o(T_v(I)) = \{h_1, h_2, \dots, h_n\} \quad (1)$$

where each hole  $h_i$  ( $i \in [1, n]$ ) is a connected components of  $H$ .

By doing so, most observed holes in  $H$  are made by nucleoli. Unfortunately, a hole may also be the space between tightly clustered nuclei. However, a hole made by a nucleolus is convex, whereas a space between clustered nuclei is not. We thus selected the subset of the holes in  $H$  whose convexity values, defined as the ratio between the volume of the hole and the volume of its convex hull, are bigger than 0.9 as the real holes that need to be filled. The value 0.9 was chosen empirically so that the number of false positives is very low.

For each hole  $h_i$  thus found, we then dilated it with a unit sphere structural element  $e$ , i.e.,  $h_i^+ = h_i \oplus e$  to get all the pixels  $h_i^+ - h_i$  surrounding  $h_i$  and then used their values to linearly interpolate intensity values for the pixels in  $h_i$ .

### 3. Adaptive thresholding

To extract the foreground mask of nuclei or clusters of nuclei, we first thresholded the image using a global background level  $t_0$  determined by Otsu's method<sup>2</sup>. Since the foreground mask  $M_0$  thus obtained contains extra background pixels at places where nuclei are tightly clustered, we then used a local adaptive thresholding to refine the mask. We first uniformly sampled the 3D image, with the sampling step along the radial and axial direction half of the radius of a typical nucleus. For each sampling pixel, we then estimated its background level<sup>2</sup> in a local window centered at that pixel and about twice of the size of a typical nucleus. Finally, using the estimated background levels at the sampling pixels as seeds, we linearly interpolated a 3D background surface of the entire 3D image stack. A pixel in  $M_0$  is set to a foreground pixel if its intensity value is higher than the background level at the same location, obtaining the final foreground mask  $M$  (Supplementary Fig. 2c).

### 4. Watershed segmentation

Once the foreground mask of clusters of nuclei has been extracted, we used the 3D watershed algorithm to separate individual nuclei<sup>3-5</sup> (Supplementary Fig. 2d). We first applied the distance transform to the foreground mask  $M$ . The distance transform of a foreground pixel in the mask is the distance between the pixel and the nearest background pixel. The resulted image is then inverted and one then applies the 3D watershed algorithm<sup>3-5</sup> to this. Briefly, watershed algorithm works in the following way. Imagine an image as a topographic relief being immersed in a lake, with holes pierced in local minima. The catchment basins, which are regions associated with these minima,

are filled up with water starting at these local minima and are successively expanded as water level increases. Dams are built at positions when water from different basins meet.

### 5. Region merging and splitting

After the above processes, most of the regions are correctly segmented. However, there were still a small number of regions over- or under- segmented, which correspond to the cases that a single nucleus was broken into pieces and that multiple nuclei were grouped together respectively. To solve these problems, we developed rule-based and training-based methods to correct segmentation errors. The rule-based method uses the statistical information of the segmented regions to predict regions of wrong segmentation and then uses rules defined on shape, size, and intensity of typical nuclei regions to do region merging/splitting. In the training-based method we trained a classifier to achieve the task (Supplementary Figs. 2e and 2f). More specifically, we first selected 2214 sample regions that fall into the three classes: correctly segmented, over-segmented, and under-segmented nuclei. Then for each sample region, we computed a vector with 25 different image features, including spatial location (3D coordinate of the gravity center of a region), size (volume of the region and the dimensions of the bounding box), intensity (mean, standard deviation, contrast, moment of inertia), and shape features (surface area, shape factor, convexity, length of major and minor axes, aspect ratio, the maximum, minimum, mean and standard deviation of the radial distance to the gravity center, as well as the ratio between the standard deviation and mean of the radial distance). After that, we selected the 4 (this number is automatically

determined) most important features using mRMR feature selection method<sup>6</sup> and used them to train a support vector machine (SVM) classifier<sup>7</sup> (with radial basis function as the kernel). The SVM does not only classify a segmented region to one of the three classes, but also provides the probability of the region falling into each class. We tested the classification accuracy using 10 fold cross validation scheme. Our results showed the trained SVM can achieve 96.85% accuracy in determine if a segmented region is correct, or should be split (under-segmented) or merged (over-segmented).

To merge over-segmented regions, we used a pair-wise hierarchical merging scheme. For each over-segmented region  $i$  identified, if it is to be merged with one of its neighboring regions  $j$ , the combined region should be predicted as a correctly segmented region. If there are multiple neighboring regions satisfying this condition, we selected the one which when merged with  $i$  will generate a region that has the highest probability of being a correctly segmented region, i.e.,  $j = \text{argmax}(P(\text{class}_{ij} = \text{'correct'}))$ . After merging the two regions, we took the combined region as a new one and repeated this process until the probability of the newly formed region being a correctly segmented nucleus region drops or it is predicted as an under-segmented region.

Under-segmented regions are usually generated by inappropriate local foreground masks which may contain extra background pixels thus making watershed algorithm fail to separate individual nuclei. To split an under-segmented region, we shrunk the foreground mask by thresholding the region at a higher background level detected by applying Otsu's method again to the pixels within the region. This usually generates a foreground mask with a better 'neck' structure so that watershed can successfully

separate nuclei. We then applied the watershed algorithm to this new foreground mask and used the merging process described above to correct over-segmentation if necessary. Since the new foreground mask generated by increasing the background level may make the nuclei smaller than their real volumes, we computed the geodesic influence zones<sup>3</sup> of the newly segmented regions in the original region mask  $U_k$  and assigned the remaining pixels in the mask (i.e.,  $p \in U_k \setminus M_k$ ) to the geodesically closest region newly segmented. Supplementary Fig. 2g shows an example of the nuclei segmentation result. Supplementary Video 1 bottom panel shows a typical image and its segmentation result in 3D.

#### 6. Annotation tool VANO and manual annotation of nuclei identities

The cross-platform 3D annotation and visualization tool VANO<sup>8</sup> (Supplementary Fig. 3) is developed in C++ and Qt. It allows experts to annotate nuclei by scrutinizing the raw image and the segmentation nuclei that are displayed side by side in 3D tri-viewed and linked together. The annotation results, including cell identities and comments, and the statistical information such as nuclear locations, sizes, gene expression levels automatically computed, are saved in a spread-sheet (Supplementary Fig. 3 lower panel). In addition to allowing experts to assign cell identities for each of nucleus in 3D, it also provides functions such as splitting, merging, and deleting existing regions and adding new regions, allowing us to evaluate automatic segmentation accuracy, and correct segmentation errors while annotating the nuclei.

We annotated nuclei identities based on the anatomy of *C. elegans* qualitatively described in earlier literatures<sup>11-12, 14-15</sup> and wormatlas<sup>13</sup> (<http://www.wormatlas.org>). The 81 body wall muscle cells and the anal depressor muscle cell (dep) were labeled by Pmyo-3::GFP so that we could identify them in GFP channel. The 81 body wall muscle cells form four essentially parallel bundles along worm body: dorsal left (21 cells), dorsal right (21 cells), ventral left (19 cells) and ventral right (20 cells). Each bundle is composed of 2 strips: medial stripe and lateral one. Nuclei of 2 stripes are intercalated along each bundle and the most anterior nuclei are medial stripes for every bundle (MusFig32, <http://www.wormatlas.org/handbook/mesodermal.htm/musclepartII.htm>). The two dorsal bundles are close to each other, so are the two ventral ones. The most posterior two ventral muscle cells are left-right symmetric while dorsal right 23, depressor muscle and dorsal left 23 form a largely straight line along anterior-posterior axis. Using these criteria, we could determine dorsal-ventral and left-right axes of a worm stack, annotate identities of the 82 GFP-expressing nuclei and then use them as landmarks to triangulate other cells. The sphincter muscle cell (sph) is located anterior, ventral and left to dep cell and usually expresses low level Pmyo-3::GFP. The two intestinal muscle (im) cells are bilaterally symmetric, usually ventral and lateral to intestine 9 right cell (int9R).

Nuclei of 20 intestine cells are located along center tube of trunk (AlimFig1, <http://www.wormatlas.org/handbook/alimentary/alimentary2.htm>). They are round with large nucleoli. In the anterior-most region a ring of four nuclei surrounds the lumen. Other eight pairs of intestine nuclei are located the lumen along the intestine tube. From int2 to int4, nuclei appear as dorsal and ventral pairs. The int5R (E.arpp) is

more ventral than int5L (E.alpp) due to the existence of gonad. But from int6 to int9 pairs, the left nucleus is more dorsal than the right one. Intestine forms a tube along the whole trunk so that annotation of intestine helps divide a worm stack into head, trunk and rectum.

Between body wall muscle ventral left and ventral right bundles, there is a ventral cord of 15 motor-neurons in trunk at L1 stage<sup>12</sup>. The most posterior nucleus (DB7) is significantly anterior to rectal neurons and InD9 and InV9.

The gonad primordium at L1 stage is in the middle of trunk, anterior to intestine and consists of four cells<sup>11</sup>. The middle two larger cells are germ cells; the two somatic cells have smaller nuclei, anterior and posterior to the germ cells, respectively. All four nuclei have relatively large nucleoli. The gonad primordium lies obliquely, with its anterior cells located slightly right and its posterior ones located slightly left.

At each side of trunk, there are four neurons, which have small nuclei<sup>11</sup>. BDU neurons are at the anterior end of trunk, surrounded by large nuclei. ALM neurons are significantly posterior and dorsal to BDU. CAN neurons are posterior and ventral to ALM, but anterior to gonad. HSN neurons are posterior to gonads.

The four Coelomocytes have small nuclei and are located to anterior part of trunk and adjacent to ventral body wall muscle bundles. Right two coelomocytes are more anterior, very close to each other<sup>11</sup>.

The 12 C lineage-derived Hyp7 nuclei, and 12 V, 12 P, and 2 Q nuclei are bilaterally symmetric<sup>11,12</sup>. Hyp7 nuclei are large nuclei with large nucleoli. They are distributed along sub-ventral part of trunk. The anterior ones (*hyp7 Caaaaa* and *hyp7 Cpaaaa*) are dorsal-posterior to BDU neurons while the most posterior ones (*hyp7 Cpappd* and *hyp7 Cpappv*) have reached rectum. V and P cells are arranged in six similar ventro-lateral pairs located on each side along the body. Relative to its V cell partner, each P cell has smaller nucleolus and is more ventral-lateral. The most anterior V cell (V1) is just posterior to BDU neuron at each side, while the most posterior P cells (P11/12) have reached rectum. Q cells are located posterior to P7/8, anterior to V5 and a little dorsal to V5. M blast cell is located at right side of trunk. It is close to QR and V5R cells, and between intestine and hypodermis layers. M cell has a large, relatively flat nucleus and a large round nucleolus.

Five AB-derived hyp7 nuclei are located laterally and just anterior to trunk<sup>11,12</sup>. They are just anterior to BUD neurons and have large nuclei with large nucleoli. Hyp7 ABarpppapa (left) and hyp7 ABarppaapa (right) are more dorsal while hyp7 ABplaapppp (left) and ABpraapppp (right) are more ventral. Hyp7 ABarpaapp is located at right side and usually posterior to hyp7 ABarpppapa and ABplaapppp. However the relative positions of the three hyp7 nuclei are not fixed. Their annotation can be indecisive in some worms.

There are seven pairs of symmetric lateral cells in the head region<sup>11,12</sup>. Here we only describe one side of a worm. Right anterior to the lateral AB-derived hyp7 is H2 blast cell, which has relative large size and a relative large nucleolus. Right anterior and

dorsal to the H2 cell is an amphid sheath cell, which has medium size and nucleolus. Right anterior and dorsal to the H2 cell is an anterior deirid sheath cell, which has small size and invisible nucleolus. The most anterior-lateral nucleus is hyp5, which has large size and large nucleolus. Posterior to hyp5 and between dorsal and ventral muscle bundle is an anterior arcade cell (arc ant DL or arc ant DR)<sup>15</sup>. H0 and H1 blast cells are located between the arcade cell and H2 cell. They have relatively large nucleus and nucleolus and arranged in anterior-posterior order.

There are nine hypodermal nuclei in the most dorsal ridge of the head, which are arranged in anterior-posterior axis<sup>12</sup>. The most anterior and dorsal cell in a worm is hyp4 ABarpapapa, followed by a pair of hyp3 nuclei. More posterior are four hyp6 nuclei, followed by two hyp7 nuclei, which have relatively large size and nucleoli.

There are seven hypodermal nuclei in anterior segment of the most ventral ridge of the head, which are arranged in anterior-posterior axis<sup>12</sup>. The most anterior and ventral cells in a worm are a pair of hyp4 nuclei, followed by an arcade cell (arc ant V)<sup>15</sup>, and then by a pair of hyp6 nuclei. More posterior are a pair of hyp7 nuclei, which have relatively large size and nucleoli.

We also annotated 12 neurons and 3 neurogenic cells in posterior segment of the most ventral ridge of the head<sup>12</sup>. These 15 cells are located between the two ventral muscle bundles. Right anterior to DB3 neuron is retrovesicular ganglion, which is composed of 12 neurons and neurogenic cell W at the anterior end. More anterior is G2 and G1 neurogenic cell.

Excretory cell has a very large nucleus with a very large nucleolus. It is located ventral and anterior to the retrovesicular ganglion<sup>12</sup>.

We annotated 86 pharynx cells. The pharynx forms a separate epithelial tube running inside the cylindrical body (Supplementary Fig. 4)<sup>14</sup>. It is more convenient to annotate pharyngeal cells from its posterior end, which is anterior to intestine.

The seven hypodermal nuclei and two T blast cells locate at the posterior end of worm<sup>12</sup>. The seven hypodermal nuclei have relatively large size. Hyp8, hyp9 and the two hyp10 nuclei are arranged at the posterior end of worm. Hyp11 nuclei are dorsal and left to hyp8 and hyp9. The two T cells have large nucleus and nucleoli and are left-right symmetric. They are anterior and dorsal to the hyp8 nucleus. The two hyp7 nuclei are anterior and ventral to the hyp8 nucleus and are located at the ventral middle line of tail.

The 36 rectal cells except muscle cells are located between intestine muscle cells and the T cells<sup>12</sup>. Cells are either left-right symmetric or located in the middle line (DD6, U, Y/PDA, F, B, DVA and DVC). The most anterior cell is PVT neuron, which is posterior to the intestine muscle cells and in the middle of left-right axis. The most posterior cell is PVR neuron, which has a small nucleus and is dorsal posterior to the T cells. The most ventral posterior cells are PLML and PLMR. They are ventral to the T cells and usually symmetric and right posterior to the T cells. However, sometimes one PLM neuron and even both two can be anterior to the T cells.

## 7. Registration

Assume we have  $K$  images  $T_1 \sim T_k$  that have been straightened, segmented, and annotated. To build the atlas, we mapped each image into a standard space so that nuclear positions are comparable. We thus used affine transform to register the  $K$  image stacks against a reference image selected from the  $K$  images. The selection of reference image is not random as we will address shortly. Assume we took  $T_i$  as the reference. To register  $T_j$  ( $j \in [1, K] \setminus i$ ) against  $T_i$ , we used the centers of the annotated nuclei in  $T_i$  and  $T_j$  as pairs of correspondence points, each pair consists of one nucleus in each image with the same cell name. Assume  $(x, y, z)$  and  $(u, v, w)$  are the 3D coordinates of one pair of correspondence points in  $T_i$  and  $T_j$  respectively. Assume  $\mathbf{A}$  is the 3D affine transform matrix, then we have:

$$\mathbf{U} = \mathbf{A} \times \mathbf{X} \quad (2)$$

$$\mathbf{U} = [u \ v \ w \ 1]^T \quad (3)$$

$$\mathbf{X} = [x \ y \ z \ 1]^T \quad (4)$$

$$\mathbf{A} = \begin{bmatrix} a_{11} & a_{12} & a_{13} & a_{14} \\ a_{21} & a_{22} & a_{23} & a_{24} \\ a_{31} & a_{32} & a_{33} & a_{34} \\ 0 & 0 & 0 & 1 \end{bmatrix} \quad (5)$$

We then derived  $\mathbf{A}$  by  $\mathbf{A} = \mathbf{U} \mathbf{X}^{-1}$ . Solving this equation needs at least 4 non-coplanar correspondence points. Since we annotated about 357 nuclei in each image, we have 357 pairs of correspondence points. Thus matrix  $\mathbf{A}$  is solved in the sense of least

square error. Using the 3D affine transform, we then mapped each  $T_j$  to a new image  $T'_j$ , which is of the same size and orientation as the reference image  $T_i$ .

To determine which image should be used as the reference, we repeated this process  $K$  times. Each time we selected one of the  $K$  images as the reference and registered the remaining ones to the selected reference. We computed the sum of the squared differences of nuclear locations of all the annotated nuclei in the registered images with respect to the reference. The image that leads to the minimum value was taken as the reference image and all the remaining images were registered to that reference.

#### 8. Statistical analysis of nuclear positions

The mean and standard deviation for each of the 357 nuclei along AP dimension have been given in Fig 2. Nuclei whose location standard deviations are more than  $\mu_{\text{std}} + 2\sigma_{\text{std}}$  along the AP axis (where  $\sigma_{\text{std}} = 0.90 \mu\text{m}$  and  $\mu_{\text{std}} = 1.87 \mu\text{m}$ ) are AMsh(L,R), ccl(1,2), ALM(L,R), HSN(L,R), 9 hyp7 nuclei, Exc gl (L,R), imL, InV(6,7), InD6, LUA(L,R), PLML, ARCAR, Exc, repD, pm1DR, vpi3V, PHshR. The mean and standard deviations along the DV and LR dimensions are further shown in Supplementary Figs. 5a and 5b. Supplementary Table 1 lists values of the mean and standard deviations of the 357 nuclei along AP, DV, and LR dimensions.

Using the mean values of the nuclear locations along AP, DV, and LR axes, we then represented each nucleus as a sphere at the corresponding locations, with the sizes of the spheres proportional to the average size of that particular nucleus across individual images. We then rendered a 3D nuclei atlas containing 357 nuclei using VANO, as

shown in Supplementary Video 2. The four bundles of the body wall muscle cells, ventral-left (VL), ventral-right (VR), dorsal-left (DL), and dorsal-right (DR) bundles, are highlighted in red, green, yellow, and blue respectively.

### 9. Computing AP/DV/LR graphs

Taking AP graph as an example, we first computed the adjacency matrix  $\mathbf{AP}_k$  for each image  $T_k$ , where  $\mathbf{AP}_k(u,v) = \text{true}$  if nucleus  $u$  is anterior to nucleus  $v$ , or either of  $u$  or  $v$  is not annotated, and  $\text{false}$  otherwise<sup>9</sup>. Then the consensus AP adjacency matrix, denoted  $\mathbf{AP}$ , can be obtained by applying the simple element-wise AND operation,  $\wedge$ , on the  $\mathbf{AP}_k$ , i.e.,  $\mathbf{AP} = \mathbf{AP}_1 \wedge \mathbf{AP}_2 \wedge \dots \wedge \mathbf{AP}_K$ . In this matrix,  $\mathbf{AP}(u,v) = \text{true}$  if and only if nucleus  $u$  is always anterior to nucleus  $v$  in all  $K$  templates, and  $\text{false}$  otherwise (we assumed that every cell name was used in at least one template). We then represented the adjacency matrix  $\mathbf{AP}$  as a graph, with each nucleus label as a node in the graph, and a directed edge from node  $u$  to node  $v$  if  $\mathbf{AP}(u,v) = 1$ . For better visualization, we then applied transitive reduction to remove the edge from  $u$  to  $w$ , if there is an edge from  $u$  to  $v$  (meaning  $u$  is anterior to  $v$ ), and an edge from  $v$  to  $w$  (meaning  $v$  is anterior to  $w$ ). Supplementary Fig. 6 shows the AP graph of all the 357 after transitive reduction. The DV and LR graphs are derived in the same way.

### 10. Adding Spatial constraints to automatic nuclei annotation

The bipartite matching scheme<sup>10</sup> does not consider the relative spatial relationships among nuclei within the subject image or within the template images. For example suppose a pair of nuclei  $(a,b)$  in the subject  $S$  should be mapped to a pair of nuclei  $(u,v)$

in the template  $T$ , with  $a$  to  $u$ ,  $b$  to  $v$ , where it is always the case that  $u$  is anterior to  $v$  in all the templates. The unconstrained bipartite matching is free to match  $a$  to  $v$  and  $b$  to  $u$  (as long as the cost is minimized) which is wrong. To solve this problem, we used invariant AP, DV, and LR relationships between nuclei to prune the potentially wrong matching edges<sup>9</sup>. For this purpose, we first derived the AP/DV/LR adjacency matrices, denoted **AP**, **DV**, and **LR** as described earlier. They represent the invariant spatial relationships between the annotated cells in templates used to build the atlas. An element in the AP matrix  $\text{AP}(u,v)=\text{true}$  if nucleus  $u$  is always anterior to  $v$  in all templates, and *false* if otherwise. The same meaning applies to **DV** and **LR**.

Given an initial matching that maps nuclei in the subject image  $S$  to nuclei in a template  $T_k$ , we constructed AP/DV/LR adjacency matrices for  $S$ , denoted **ap**, **lr**, and **dv**. Take the **ap** matrix as an example, we set an element in  $\text{ap}(u,v) = \text{true}$  if  $a$  is mapped to  $u$  and  $b$  is mapped to  $v$ , and nucleus  $a$  is anterior to nucleus  $v$  in the subject image  $S$ .

Using these adjacency matrices, we then computed a conflict matrix **C**. An element  $\mathbf{C}(u,v)$  equals *true* if the spatial relationship along AP, or DV, or LR in the templates and in the subject image are contradictory. Mathematically, **C** is computed in the following way:

$$\mathbf{C} = \mathbf{C}_{\text{ap}} \vee \mathbf{C}_{\text{lr}} \vee \mathbf{C}_{\text{dv}} \quad (6)$$

$$\mathbf{C}_r = [(\mathbf{R}) \wedge (\neg \mathbf{R}^T) \wedge (\neg \mathbf{r}) \wedge (\mathbf{r}^T)] \vee [(\neg \mathbf{R}) \wedge (\mathbf{R}^T) \wedge (\mathbf{r}) \wedge (\neg \mathbf{r}^T)] \quad (7)$$

where  $\vee, \wedge, \neg$  are the element-wise OR, AND, and NOT operations, respectively, and  $T$  is matrix transposition.  $\mathbf{R}$  represents adjacency matrices  $\mathbf{AP}$ ,  $\mathbf{LR}$ ,  $\mathbf{DV}$ , and  $\mathbf{r}$  represents adjacency matrices  $\mathbf{ap}$ ,  $\mathbf{lr}$ ,  $\mathbf{dv}$  respectively. Moreover, when  $\mathbf{r}$  equals say  $\mathbf{ap}$  in Eq. (7) then  $\mathbf{R}$  is  $\mathbf{AP}$ . Observe that  $\mathbf{C}(u,v) = \text{true}$  if and only if one or more of the AP, LR, or DV relationships of nuclei  $a$  and  $b$  in the subject image are contradictory to those of nuclei  $u$  and  $v$  in the template. Thus at least one of  $a$  and  $b$  is wrongly recognized.

Using the conflict matrix  $\mathbf{C}$ , we counted, for each nucleus  $a$  to be recognized in the subject image  $S$ , the number of nuclei in  $S$  that have a contradictory AP/LR/DV relationships with nucleus  $a$ , i.e.,

$$\text{conflict}(a) = |\{b \mid \mathbf{C}(u,v) = 1, a \rightarrow u, b \rightarrow v\}| \quad (8)$$

We then selected, with high confidence, the nucleus in the subject image  $S$  that had the maximum number of conflicted nuclei as the one that had been wrongly labeled by the current matching. We then removed the edge between this nucleus in  $S$  and its mapped nucleus in the template  $T_k$  and rerun the bipartite matching. This process is repeated until  $\sum_a \text{conflict}(a)$  does not decrease for  $t_{\max}$  sequential steps ( $t_{\max}=3$  for the results reported, but other values yielded similar results.). Once terminated, one takes as the answer the matching that gives the minimum  $\sum_a \text{conflict}(a)$ .

## References for Supplementary Note

1. Peng, H., Long, F., Liu, X., Kim, S., Myers, E., (2008) Straightening *C. elegans* images. *Bioinformatics* 24, 234-242.
2. Otsu, N. (1979) Threshold Selection Method from Gray-Level Histograms. *IEEE Transactions on Systems, Man, and Cybernetics* 9, 62-66.
3. Vincent, L. and Soille, P. (1991) Watersheds in digital spaces: an efficient algorithm based on immersion simulations. *IEEE Trans. Pattern Analysis and Machine Learning* 13 (6), 583-598.
4. Beucher, S., Meyer, F. (1993) *Mathematical Morphology in Image Processing* (E.R. Dougherty ed.) New York: Marcel Dekker 433.
5. Meyer, F., (1994) *Signal Processing* 38,113.
6. Peng, H., Long, F., Ding, C. (2005) Feature selection based on mutual information: criteria of max-dependency, max-relevance, and min-redundancy. *IEEE Transactions on Pattern Analysis and Machine Intelligence* 27, 1226-1238.
7. Burges, C. J. C. (1998) *Data Mining and Knowledge Discovery* 2,121.
8. Peng, H., Long, F., and Myers, G. (2009) VANO: a volume-object image annotation system. *Bioinformatics* 25(5), 695-697.
9. Long F., Peng, H., Liu, X., Kim, S., and Myers, E (2008) Automatic recognition of cells (ARC) for 3D images of *C. elegans*. *Lecture Notes in Computer Science* 4955, 128-139.

10. Cormen, T.H., Leiserson, C.E., Rivest R.L., and Stein C. (2001) *Introduction to algorithms* (second edition, MIT Press and McGraw-Hill).
11. Sulston, J.E., and Horvitz, H.R. (1977). Post-embryonic cell lineages of the nematode, *Caenorhabditis elegans*. *Developmental biology* 56, 110-156.
12. Sulston, J.E., Schierenberg, E., White, J.G., and Thomson, J.N. (1983). The embryonic cell lineage of the nematode *Caenorhabditis elegans*. *Developmental biology* 100, 64-119.
13. Hall, D. H., Altun, Z. F. (2007) *C.elegans atlas*. (Cold Spring Harbor Laboratory Press).
14. Albertson, D.G., and Thomson, J. N. (1976). The pharynx of *Caenorhabditis elegans*. *Philosophical transactions of the royal society of London* 275, 299-325.
15. Wright, K.A., and Thomson, J. N. (1981). The buccal capsule of *C.elegans* (Nematoda: Rhabditoidea): an ultrastructural study. *Canadian Journal of Zoology* 59, 1952-1961.